

A Study on MIMO Mobile-To-Mobile Wireless Fading Channel Models

Submitted in accordance with the requirements for the degree of the Erasmus Mundus Master
of Science in Computer Vision and Robotics (ViBot)



HERIOT WATT UNIVERSITY



School of Engineering And Physical Sciences

June 2008

By:

Luis Alfredo Mateos Guzman

(06226154)

Table of Contents

Declaration	3
Acknowledgement	4
Abstract	5
List of Figures	6
List of Tables	7
List of Symbols	8
Abbreviation	10
1 Introduction	
1.1 Aims and Objectives	11
1.2 Background Information	11
1.2.1 What is a Multiple Input Multiple Output (MIMO) system	11
1.2.2 What is a Mobile to Mobile (M2M) communication channel	14
1.2.3 MIMO M2M channel modelling	14
1.2.4 The need for accurate MIMO M2M channel models	15
2 Literature review	
2.1 Classification of MIMO M2M Channel Models	17
2.1.1 Physical Models	18
2.1.2 Analytical Models	19
2.2 MIMO M2M Geometric-Based Stochastic Model (GBSM)	21
2.3 The MIMO M2M Geometric Elliptical Model	22
2.3.1 Properties of the MIMO M2M Geometric Elliptical Model	23
2.3.2 Space Time (ST) Correlation Function (CF)	24
2.3.3 Space Doppler (SD) Power Spectral Density (PSD)	25
2.3.4 Level Crossing Rate (LCR)	26
2.3.5 Average Fade Duration (AFD)	27
3 A Mathematical representation of the MIMO M2M Geometric Elliptical Model	
3.1 Determining the MIMO M2M Elliptical Model Properties	28
3.2 The MIMO M2M Elliptical Reference Model	29

3.3	MIMO M2M Mathematical Representation	32
3.3.1	ST CF and SD PSD	35
3.3.1.1	ST CF	35
3.3.1.2	SD PSD	37
3.3.2	LCR and AFD	37

4 Results and analysis of the MIMO M2M Statistical Properties

4.1	Space Doppler frequency Power Spectral Density	39
4.1.1	SD PSD in isotropic scattering environment	39
4.1.2	SD PSD in non isotropic scattering environment	40
4.1.3	SD PSD moving in the same directions	41
4.1.4	SD PSD moving in opposite directions	42
4.2	Level Crossing Rate and Average Fading Duration	43
4.2.1	LCR and AFD $k_T = k_R = 0$ isotropic scattering environment	44
4.2.2	LCR and AFD $k_T = k_R = 3, \mu_T = 0, \mu_R = \pi$ non isotropic environment	45
4.2.3	LCR and AFD $k_T = k_R = 3, \mu_T = \mu_R = \pi / 2$ non isotropic environment	46
4.3	LCR and AFD of the MIMO M2M model for different Ricean factors	47
4.3.1	LCR and AFD $k_{pq} = 0$ non isotropic environment	47
4.3.2	LCR and AFD $k_{pq} = 1$ non isotropic environment	48
4.3.3	LCR and AFD $k_{pq} = 5$ non isotropic environment	49

5 Conclusion and future work

5.1	Conclusion	50
5.2	Future work	50
	References	51
	Appendices	54

"I Luis Alfredo Mateos Guzmán confirm that this work submitted for assessment is my own work and is expressed in my own words. Any uses made within it of the words of other authors in any form e.g., ideas, equations, figures, text, tables, programs, etc., are properly acknowledged. A list of references employed is included"

Luis Alfredo Mateos Guzman

Acknowledgement

My grateful thanks to my supervisor, Dr Cheng-Xiang Wang, for his support throughout my Master Thesis semester of study and to Xiang Cheng, whose generous suggestions helped make changes and improvements in this Master Project.

Abstract

Mobile-to-Mobile (M2M) communications applications can be seen in mobile ad-hoc networks, wireless sensor networks, and intelligent transport systems, these systems require direct communication between a mobile transmitter and a mobile receiver over a wireless medium. Such Mobile-to-Mobile communication systems differ from the conventional cellular radio systems, where the Base Station is stationary and only the Mobile Station is moving.

The employment of multiple antennas at both the transmitter and receiver, known as Multiple Input Multiple Output (MIMO) technologies, enables to greatly improve the link reliability and increase the overall system capacity. For the design and test of such MIMO Mobile-to-Mobile systems, we need to have a thorough understanding and an accurate modelling of the underlying channels. For this purpose, the Geometrically-Based Stochastic Model (GBSM) has been applied for narrowband MIMO Mobile-to-Mobile channel modelling. The most important GBSMs include the one-ring model, two-ring model and Elliptical-ring model, in which the Elliptical-ring model is predestinated for modelling either narrow and wideband MIMO channels in microcellular and picocellular environments.

In this project, the statistical properties of narrowband MIMO Mobile-to-Mobile wireless fading channels in non-isotropic scattering environments will be investigated in detail based on the elliptical-ring model. The interested properties include Space-Time-Frequency Correlation properties, Space-Doppler-frequency Power Spectral Density, Level Crossing Rate, and Average Fading Duration.

List of Figure

- 1.1 A MIMO system with multiple antennas in both transmitter and receiver.
- 1.2 A MIMO M2M time variant channel based on the Elliptical-ring model.
- 2.1 Classifications of MIMO channel and propagation models.
- 2.2 Level Crossing Rate (LCR) threshold.
- 2.3 Average Fade Duration (AFD) fade and non-fade periods for a sample of a fading signal.
- 3.1 Geometric elliptical scattering model for a MIMO M2M channel with local scatterers $S(n)$ lying on an ellipse.
- 3.2 Geometric elliptical scattering model for a wideband MIMO M2M channel with multiple clusters of scatterers $S(n)$ lying on an ellipse.
- 3.3 Geometric elliptical scattering model for a wideband MIMO M2M channel with Multiple clusters of scatterers $S(n)$ lying on L ellipses.
- 3.4 A Tapped Delay line model for discrete multipath channels.
 - 4.1.1 SD PSD $k_T = k_R = 0$ isotropic scattering environment.
 - 4.1.2 SD PSD $k_T = k_R = 1, \gamma_T = 0, \gamma_R = \pi$, non isotropic scattering environment moving in opposite directions.
 - 4.1.3 SD PSD $k_T = k_R = 1, \gamma_T = 0, \gamma_R = 0$, non isotropic scattering environment moving in the same directions.
 - 4.1.4 SD PSD $k_T = k_R = 3, \gamma_T = 0, \gamma_R = \pi$, non isotropic scattering environment moving in opposite directions.
 - 4.2.1 LCR and AFD $k_T = k_R = 0$ isotropic scattering environment.
 - 4.2.2 LCR and AFD $k_T = k_R = 3, \mu_T = 0, \mu_R = \pi$ non isotropic scattering environment.
 - 4.2.3 LCR and AFD $k_T = k_R = 3, \mu_T = \mu_R = \pi / 2$ non isotropic scattering environment.
- 4.3.1 LCR and AFD $k_{pq} = 0$ and $(k_T = k_R = 1, \gamma_T = 0, \gamma_R = \pi)$ non isotropic scattering environment.
- 4.3.2 LCR and AFD $k_{pq} = 1$ and $(k_T = k_R = 1, \gamma_T = 0, \gamma_R = \pi)$ non isotropic scattering environment.
- 4.3.3 LCR and AFD $k_{pq} = 5$ and $(k_T = k_R = 1, \gamma_T = 0, \gamma_R = \pi)$ non isotropic scattering environment.

List of Tables

- 1.1 History of 3G MIMO techniques.

List of Symbols

K_R^{SB}	Angle spread of the AoA
δ_R	Antenna element spacing at Rx
δ_T	Antenna element spacing at Tx
ϕ_{Rq}^{LoS}	AoA of a LoS path.
$\phi_R^{(n)}$	AoA of the waves traveling from the effective scatterers towards the Rx
$\phi_T^{(n)}$	AoDs of the waves that impinge on the effective scatterers
$(\cdot)^*$	Complex conjugate operation
$\delta(\cdot)$	Dirac delta function
ε_{pq}	Distances of the relevant angles
f_D	Doppler frequency
$S_{TR}^{(n)}$	Effective scatterer
$Q(\cdot, \cdot)$	Generalized Marcum Q function
$f_{R\max}$	Maximum Doppler frequencies in Rx
$f_{T\max}$	Maximum Doppler frequencies in Tx
μ_R^{SB}	Mean value of AoA
β_T	Multi-element Tx antenna tilt angles
β_R	Multi-element Rx antenna tilt angles
$h_{pq}(t)$	Received complex impulse response
K_{pq}	Ricean factor
γ_R	Rx angle of motion
V_R	Rx speed
Ω_{pq}	Total power
γ_T	Tx angle of motion
V_T	Tx speed
a	Semimajor axis of the ellipse
b_1^{SB}	Spectral moments for the single bounced component

- b_2^{SB} Spectral moments for the single bounced component
- c Speed of light
- $E[\cdot]$ Statistical expectation operator
- τ_{pq} Wave propagation velocity

Abbreviation

AFD	Average Fade Duration
AoA	Angle of Arrival
AoD	Angle of Departure
APS	Angular Power spectrum
BS	Base Station
CF	Correlation Function
F2M	Fixed to Mobile
LCR	Level Crossing Rate
LoS	Line of Sight
DoA	Direction of Arrival
DoD	Direction of Departure
MIMO	Multiple Input Multiple Output
MPC	Multi-Path Component
MS	Mobile Station
M2M	Mobile to Mobile
OFDM	Orthogonal Frequency-Division Multiplexing
PDF	Probability Density Function
PDP	Power Delay Profile
PSD	Power Spectral Density
Rx	Receiver
SD	Space Doppler
ST	Space Time
TDoA	Time Delay of Arrival
Tx	Transceiver
3G	Third Generation Mobile

1 Introduction

1.1 Aims and objectives

The aim of this project is to study the statistical properties of narrowband MIMO Mobile-to-Mobile wireless fading channels in non-isotropic scattering environments based on the Elliptical-ring model. The interested properties include Space-Time-Frequency Correlation properties, Space-Doppler-frequency Power Spectral Density, Level-Crossing Rate, and Average Fading Duration.

The results of the comparison of the results obtained will be used to determine the effectiveness of the modelling technique, its practical advantages and disadvantages.

1.2 Background Information

1.2.1 What is a Multiple Input Multiple Output (MIMO) system

The Multiple Input Multiple Output (MIMO) systems are equipped with multiple antennas, at both the transmitter and receiver in order to improve communication performance, in contrast to conventional communication systems with only one antenna on the transmitter and one antenna on the receiver.

A MIMO system offers significant increases in data throughput and link range without additional bandwidth or transmit power. It achieves this by higher spectral efficiency (more bits per second per hertz of bandwidth) and link reliability or diversity (reduced fading) [15]. These MIMO characteristics are essential for the coming generation of Telecommunications systems.

MIMO channels are commonly called vectorial channels because for each transmit-receiver pair a channel is established. In the next figure is easy to observe this relationship.

For the transmitter **Tx**, the antenna Tx1 will have a vectorial channel h_{11} to the receiver **Rx** in the antenna Rx1; the antenna Tx1 will have a vectorial channel h_{21} to the receiver antenna Rx2; the antenna Tx1 will have a vectorial channel h_{31} to the receiver antenna Rx3 and so on.

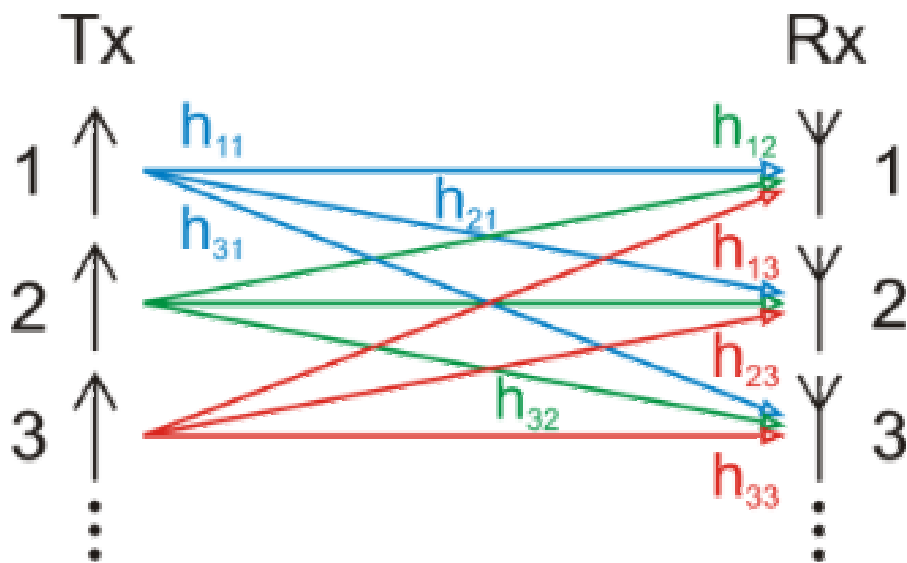


Figure 1.1 A MIMO System with Multiple Antennas in both transmitter and receiver.

In this third generation (3G) of mobile phone standards and technology, the 3G enable network operators to offer users a wider range of more advanced services while achieving greater network capacity through improved spectral efficiency. Services include wide-area wireless voice telephony, video calls, and broadband wireless data, all in a mobile environment.

Generation	3G	3G evolution
Time scale	2003/4	2005~6/2007~8/2009~10
Standard	WCDMA	HSPA/HSPA+/LTE
Total rate	384kbps	14/42/65~250Mbps
Bandwidth	5MHz	5MHz/20MHz
Requirement Paradigm	High reliability (High quality)	High rate (High capacity)
Method	Spatial diversity	Spatial multiplexing
Spatial coding (SC)	Spatial diversity coding	Spatial multiplexing coding
Spatial beamforming (SB)	Single-stream beamforming	Multi-stream beamforming
Examples	SC: Alamouti coding, SB: TxAA	SC: BLAST coding, SB: SVD

Table 1.1 History of 3G MIMO techniques.

MIMO is a method of transmitting and receiving two or more unique data streams through a single radio channel, increasing the maximum data rate achievable on every single radio channel.

By applying MIMO technology, we can directly take advantage of 2 very important properties;

- a. Diversity
- b. Multiplexing.

Diversity means that the system provide a receiver with multiple replicas (copies) of the same information bearing signal, the duplicated signals are slightly changed by fading. The 3 types of Diversity techniques are:

I. Space Diversity

This means the antenna elements are sufficiently spaced apart to achieve independence between the transmitted and received signals. The spatial separation needs to be at least half the wavelength to obtain desired results of independence [16].

II. Time Diversity – without wasting bandwidth

The same information is transmitted in different Time slots with the time slots separated by measures equal to or greater than the coherence time of the channel.

III. Frequency Diversity

The same information is transmitted on different carrier frequencies which are separated by measures equal to or greater than the coherence bandwidth of the channel.

The reliability of the network is improved by taking advantage of the space and time diversity while the rate of transmission is improved by multiplexing.

MIMO can be used with any modulation or access technique, and it has been further improved by using a technique called Orthogonal Frequency Division Multiplexing (OFDM), through which we can divide the frequency selective channel into many flat fading channels and then apply the MIMO transmit/receive techniques to each of these sub-channels[9].

1.2.2 What is a Mobile to Mobile (M2M) communication channel

In Mobile-to-Mobile (M2M) communication channels, both the transmitter and the receiver are in motion. For example, one vehicle in a given location of a city tries to communicate to other moving vehicle in other location. This can be a police cars, emergency vehicles or military in certain an events.

In this situations were the vehicles are inside a city, the Line-of-Sight is often obstructed by buildings or any other type of obstacle between the transmitter and the receiver, these obstacles can be scatterers or any other mechanisms that diffract or reflect the signal.

A Mobile-to-Mobile propagation model is needed to evaluate mobile to mobile communication systems. The major difference between Mobile-to-Mobile and the Mobile-to-Base lies mainly in the location of the antennas, their heights and the surrounding scatterers. The proposed propagation model is based on a time variant channel.

1.2.3 MIMO M2M channel modelling

The radio propagation channel determines crucial MIMO M2M system characteristics. Therefore the modelling of MIMO M2M channels plays the most important part for MIMO M2M system design, simulation and deployment. The modelling of a channel is an attempt to develop a mathematical model that describes a channel, the response to different input conditions, the behaviors, and determine its mathematical representation.

In channel modelling there are two key points, Accuracy and Efficiency.

Accuracy measures the quality of the model and Efficiency determines the complexity of the model. In order to obtain a balance there must be a trade-off between both, because the more accurate a model is, the more complex and less efficient. In the other hand, the more efficient a model is, the less accurate; because it will take into account the generalities of the channel and forget about the details of it.

In order to create a balance it is necessary to make some assumptions, for example, the scatterers (the objects in the environment that may act as obstacles in the path of signal) in the Elliptical model exists along the Ellipse because this simplifies and create the model understandable.

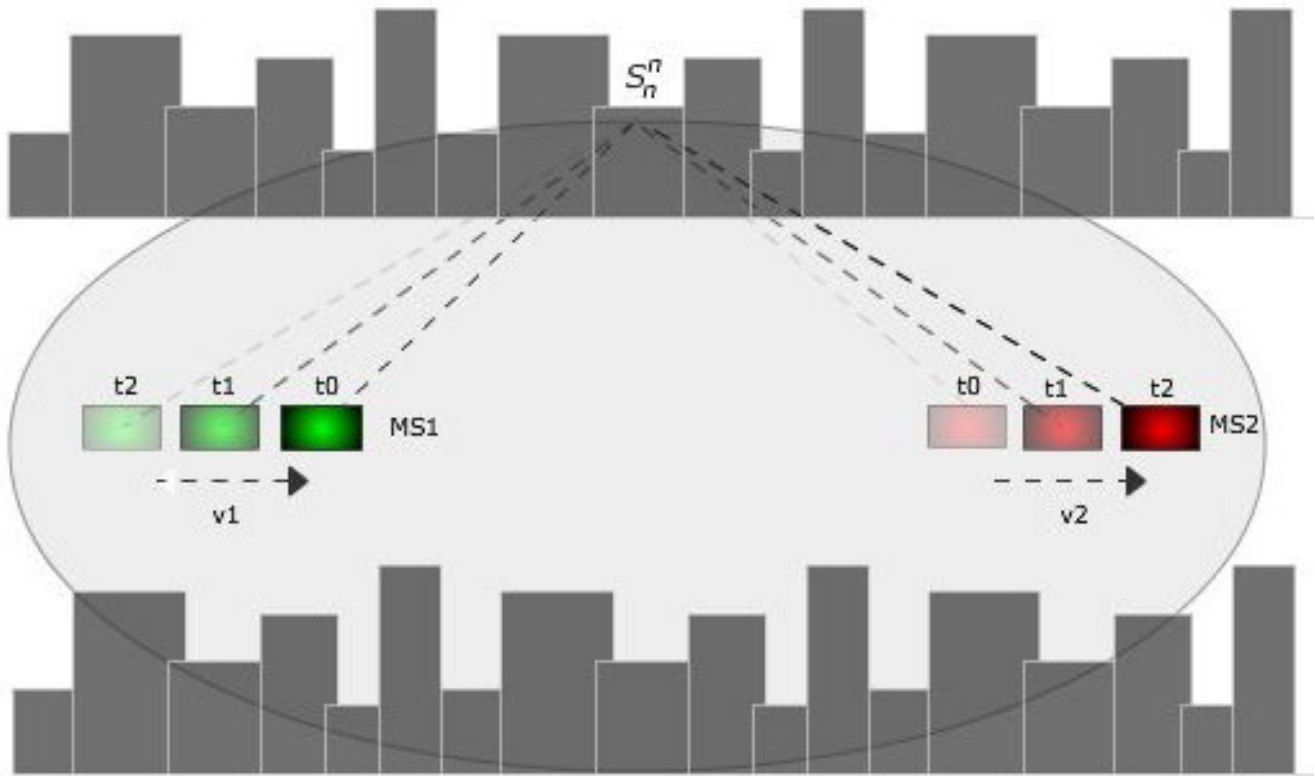


Figure 1.2 A MIMO M2M time variant channel based on the Elliptical-ring model.

1.2.4 The need for accurate MIMO M2M channel models

The modelling of MIMO channel needs to be accurate and practical. Given that the propagation conditions of a channel greatly determine its capacity expected for a MIMO system, we need practical channel simulation techniques to describe and model the MIMO channel for different conditions so we can predict, simulate and design high-performance communication systems [7], and MIMO channels need to be described for all transmit and receive antenna pairs [7].

In MIMO systems, the propagation of electromagnetic waves from a transmitter to a receiver is characterized by the presence of multi-paths due to various phenomena such as reflection, refraction, scattering and diffraction and the performance of MIMO systems is largely dependent on the propagation medium [17].

Valid MIMO communication systems models can help in reducing the costs of research and development by simplifying the required measurements on the design, and improving the

modulation schemes under different scenarios and system performances can be accurately predicted.

Therefore, accurate modelling of MIMO channels is an important prerequisite for MIMO M2M system design, simulation, and deployment.

In order to introduce the subject topic, I will start by defining the different classification methods of MIMO M2M channels; MIMO M2M channel models can be divided into the wide band models and the narrow band models directly by considering the bandwidth of the system [8]. The wideband models consider the propagation channel to be frequency selective, which means that different frequency sub-bands have different channel responses while on the other hand, the narrow band models assume that the channel has frequency non-selective fading and therefore, the channel has the same response over the entire system bandwidth [8].

In this project I intend to determine the statistical properties of narrowband MIMO M2M wireless fading channels in non-isotropic scattering environments based on the elliptical-ring model. And investigate the interested properties include Space-Time-Frequency Correlation properties, Space-Doppler-frequency Power Spectral Density, Level-Crossing Rate, and Average Fading Duration.

To achieve this MIMO M2M model, there will be two stages, the first would be to derive the mathematical representation of the Reference model and the statistical properties, the second would be to carry out simulations and comparisons using MATLAB.

In these simulations and comparisons, I intend to show that having a clear understanding of the statistical properties of the MIMO M2M Elliptical channel model, it is possible to adequately describe its behaviors and important parameters

2. Literature review

MIMO M2M technology plays a very important role in future of wireless telecommunications, therefore, in order to design and determine the performance of MIMO M2M wireless communication systems, it is very important to have accurate and realistic models of the propagation channel.

An antenna array can be described as a Spatio-Temporal filter, which takes advantage of both time-domain and space-domain signal characteristics [18]. According to the wireless connection scheme between a Mobile Station1 (MS1) and a Mobile Station2 (MS2) in macro cells, both stations are surrounded by scatterers that may give rise to different modes of signal propagation toward the user.

The use of antenna arrays for wireless cellular systems is continually increasing, as they improve the coverage and quality of such systems by combating interference and fading, and by using antenna arrays at both transmitters and receivers, the capacity of wireless channels can be increased significantly [18].

Some more information on the different geometries defining the relationship between the MS1, MS2 and Scatterers, is given below.

2.1 Classification of MIMO M2M channel models

MIMO M2M Channels may be classified into either of the following types, Narrowband (i.e. Flat-fading) or Wideband (Frequency-selective) models; Time-varying or Time-invariant models; and as Physical or Analytical models [7].

The model selected should take into consideration the wideband characteristics as well as the Space-Time-Frequency domain properties. The influence of the measurement equipment (bandwidth, antenna array type, heights of antennas, etc.) must be excluded from the channel; thus, a physical model is preferred [9].

In this project, I intend to work with the physical models, in specific the Elliptical model, the main reasons for this choice are explained below.

2.1.1 Physical Models

Physical channel models characterize an environment on the basis of electromagnetic wave propagation by describing the double-directional multipath propagation, between the location of the transmit (Tx) array and the location of the receive (Rx) array [7].

They clearly model wave propagation parameters like the complex amplitude, Direction of Departure (DoD), Direction of Arrival (DoA), and delay of a Multi-Path Component (MPC) [7]. They also consider the distributions of some other very important physical parameters that can be used to describe a realistic MIMO M2M channel, such as the Time Delay of Arrival (TDoA), and Doppler shift [9].

More sophisticated models also incorporate polarization and time variation. Depending on the chosen complexity, physical models allow for an accurate reproduction of radio propagation [7]. Physical models are independent of antenna configurations (antenna pattern, number of antennas, array geometry, polarization, mutual coupling) and system bandwidth. Physical MIMO M2M channel models can further be split into Deterministic models, Geometry-Based Stochastic models, and Non-Geometric Stochastic models [7].

The channel impulse response in the deterministic models is obtained by tracing the reflected and scattered rays, this type of model also have the advantage of being able to generate accurate site specific and easily reproducible information.

Stochastic models, describe the characteristics of the radio channel by means of the joint Probability Density Function (PDF) statistical parameters employed in such models, usually estimated from extensive measurements.

Here are some of the main characteristics for each of these model types.

a. Deterministic Models

Deterministic models characterize the physical propagation parameters in a completely deterministic manner (examples are Ray Tracing and Stored Measurement Data).

b. Geometry-Based Stochastic Models

With Geometry-based Stochastic Channel Models (GBSM), the impulse response is

characterized by the laws of wave propagation applied to the specific Tx, Rx, and scatterer geometries, which are chosen in a stochastic (random) manner.

c. Non-Geometrical Stochastic Models

The non-geometric stochastic models describe and determine physical parameters (DoD, DoA, delay, etc.) in a completely stochastic way by prescribing underlying probability distribution functions without assuming an underlying geometry (examples are the extensions of the Saleh-Valenzuela model) [20] [21].

2.1.2 Analytical Models

In contrast to physical models, analytical channel models characterize the impulse response (equivalently, the transfer function) of the channel between the individual transmit and receive antennas in a mathematical - analytical way without explicitly accounting for wave propagation. Analytical models are very popular for synthesizing MIMO matrices in the context of system and algorithm development and verification.

Analytical models can be further subdivided into Correlation-based models and Propagation-motivated models.

a. Correlation-based Models

Correlation-based models characterize the MIMO channel matrix statistically in terms of the correlations between the matrix entries [7]. Most commonly used correlation-based analytical channel models are the Kronecker model [22], [23], [24], [25] and the Weichsel Berger model [26].

b. Propagation-motivated Models

Propagation-motivated models describe the MIMO channel matrix via propagation parameters [7]. Examples are the finite Scatterer model, the maximum entropy model, and the virtual channel representation [7].

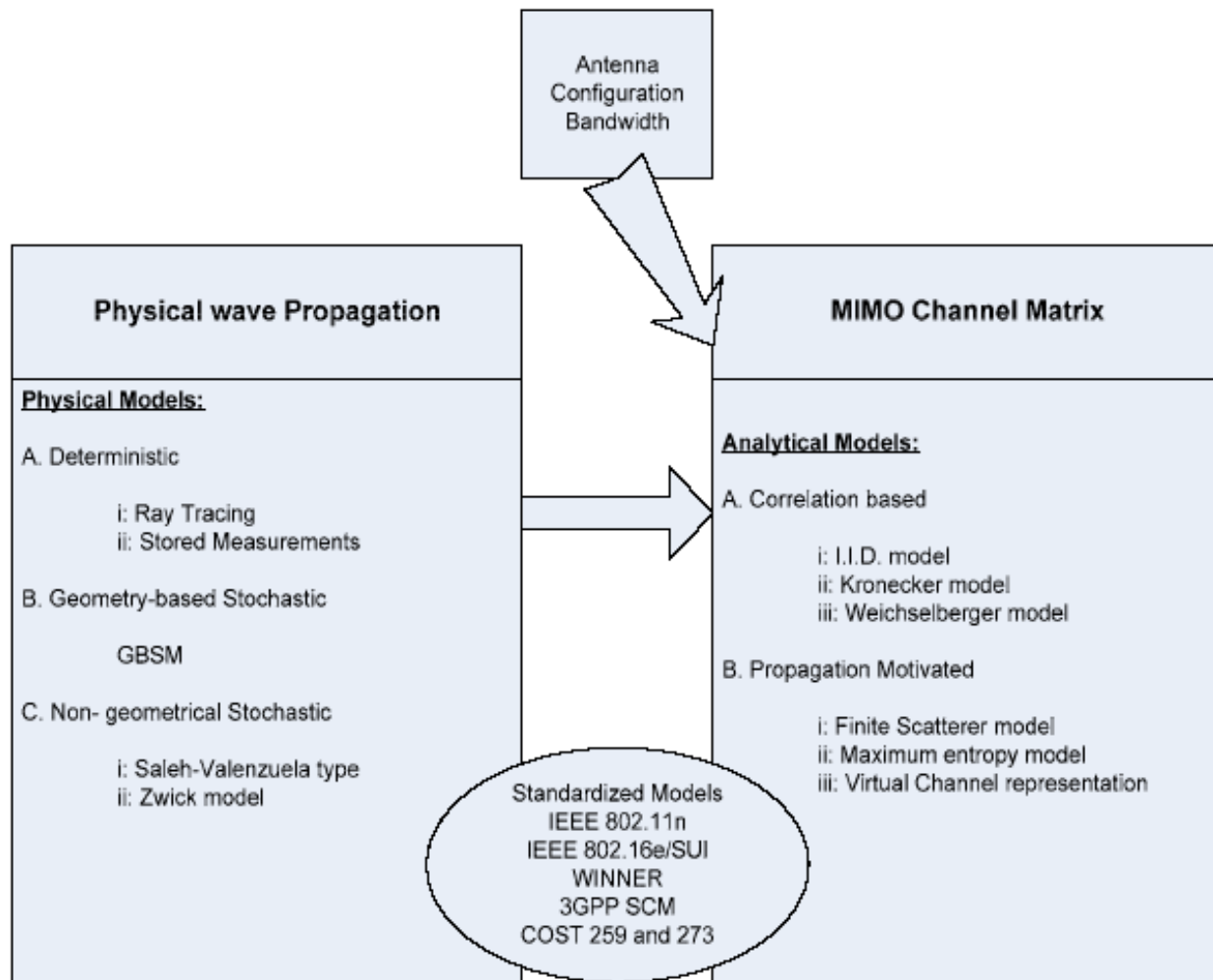


Figure 2.1 Classifications of MIMO Channel and Propagation Models

2.2 MIMO M2M Geometric-Based Stochastic Model (GBSM)

For any geometrically-based channel model, the signal statistics depends on the position of the Mobile Station1 (MS1), Mobile Station2 (MS2) and the geometrical distribution of the scatterers around the two Mobile Stations.

In order to simplify the derivation of the channel expression it is necessary to make 2 important assumptions.

1. The signal goes through 1 reflections at least as it travel from the MS1 to the MS2.
2. The scatterers are confined within a scattering region.

There are three basic Geometric Channel model representations

- a. The one-ring model
- b .The two-ring model
- c .The Elliptical model

a. The One-ring model

The One-ring model is preferred in modelling sub-urban environments where the base station BS and the mobile station MS are considerably distant from each other and the BS is at a height much higher than the MS. In this type of environment, the BS has little or no scatterers surrounding it, as it is placed on a very elevated point, (e.g. a hill or mountain or Tower), while the MS, at a much lower point, (e.g. average human height), is surrounded by many scatterers assumed to exist on a ring around the MS.

This One-ring model in the case of a Mobile-to-Mobile communication system may be seen as an airplane or helicopter communicating with a ground vehicle.

b. The two-ring model

The Two-ring model is similar to the One-ring model; the difference being the height/vertical position of the BS, which is not as high as that in the One-ring model, thus permitting the assumption that the BS is surrounded by scatterers existing on a ring too. Therefore, we have Two rings, one surrounding the BS and the other the MS, where scatterers exist.

This model in the case of Mobile-to-Mobile communications may be seen as a helicopter flying low in the city communicating with a ground vehicle.

c. The Elliptical model

In the Elliptical Model, the MS1 and MS2 are closer to each other, and are placed at about the same vertical heights, and the scatterers exist on the ellipse surrounding both the MS1 and MS2, each positioned at the focal points of the Ellipse.

A GBSM has the following important advantages [7]:

1. It can be applied to physical/real conditions;

This is because important parameters (like the scatterer locations) can often be determined using simple geometrical considerations;

2. Many effects are implicitly reproduced;

Small-scale fading is created by the superposition of waves from individual scatterers, DoA and delay drifts (from Doppler shifts) as a result of the MS movement are also taken into consideration;

3. All information is dependent on the distribution of the scatterers;

Therefore, dependencies of Power Delay Profile (PDP) and Angular Power spectrum (APS) do not lead to a complication of the model;

4. Tx/Rx and scatterer movement as well as shadowing and the (dis)appearance of propagation paths (e.g. due to blocking by obstacles) can be easily implemented;

This allows us to include long-term channel correlations in a straightforward way.

2.3 The MIMO M2M Geometric Elliptical Model

The Geometrical Elliptical Scattering Model has definitive properties which can be described by using its correlation functions. The correlation functions describe the basic components of the MIMO M2M communication system by its spatial, temporal and frequency characteristics. By analyzing the correlation functions is easier to investigate the potential of the MIMO M2M wireless communication systems.

These basic components do not always have solutions that can be expressed clearly in terms of a bounded number of elementary functions, such as addition, subtraction, multiplication, division, square root, etc. In other words, they do not always have closed form expressions. Hence, in such cases, we may use assumptions and use the Von Mises Probability Density Functions to suggest closed form solutions.

In this project, the analysis of the Geometrical Elliptical model is 3 dimensional (3D), describing the Spatial, Temporal, and Frequency characteristics of the MIMO M2M system. Each of these components has a very important part to play in expressing the effects of the Mobile Station1, Mobile Station2, and the propagation environment on the correlation functions.

2.3.1 Properties of the MIMO M2M Geometric Elliptical Model

The MIMO M2M Elliptical Model is an example of a Geometric-Based Stochastic Model , and is preferred over the One-ring and Two-ring models, because while the latter models are used primarily to represent Narrow-band MIMO channels [17], the Elliptical model can be used to represent either narrow or wideband MIMO channels. The Frequency-selectivity feature of the Elliptical model also makes it the preferred choice for developers of future mobile communication systems [17].

As explained before the Geometric Elliptical model was originally proposed for spatial channels in micro and pico - cell environments, where the antenna heights are low, at ground level, so that multipath scattering is just as likely near the mobile station 1 as it is near the mobile station 2.

The Elliptical model has the physical interpretation that only multipath components with time delay smaller than the specified maximum time delay are considered.

The following parameters are defined in the figure 3.1,

- a. The distance between the MS1 and MS2.
- b. The distance between the MS1 (MS2) to the local scatterers along the ellipse.

c. The various angles defined by the relationship between different points with the elliptical region.

It can be deduced, as earlier mentioned, that a 3D MIMO propagation environment is affected by Space, Time and Frequency and we will attempt to model the various effects of each property. For example, assuming we have 2 antennas each at both Transmit and Receive ends, and both antennas use the same carrier frequency, their relative distance, vertical separation and different heights will affect the modelling function [17].

Spatial properties

The spatial properties are well defined by the Time delay experienced between the Tx transmitter and Rx receiver antennas, and the speed of wave propagation (the speed of light c).

Frequency correlation properties

In MIMO M2M channel modelling, it is important take into consideration the several issues that affect propagation within the channel like variation in time, multipath phenomena and Doppler shifts, angle of arrival of the received signals, and also the effects of using multiple carrier frequencies [7].

The correlation between the frequency properties decreases when the frequencies or their differences increase. The proposed 3D model takes into account the antenna heights. The vertical separation of antenna elements is the result of their different heights. Such a difference in the antenna heights produces phase differences between the received or transmitted signals and consequently impact on the correlation function. This property can be employed to improve the space diversity in wireless systems [17].

Next, I intend to show how the physical properties of the wireless communication channel listed below should be modelled.

2.3.2 Space Time (ST) Correlation Function (CF)

In a MIMO M2M wireless system, the transmitted signal in the channel has a complicated interaction with the environment. There are reflections and refractions likely to occur from

large objects, diffraction of the electromagnetic waves around objects, and signal scattering. The result of these complicated interactions is the presence of many signal components, differing paths of reception or multipath signals, at the receiver [2], which can be described using their Space, Time and Frequency properties.

Performing a correlation of these properties gives a more in-depth and accurate description of the MIMO M2M channel model, and I will start by reviewing the Space-Time Correlation properties, the Frequency Correlation properties, then the Space-Doppler-frequency Power Spectral Density, Level Crossing Rate and Average Fading Duration.

Previous work on this subject has proven that accurate models should take sufficient consideration of the physical geometry of scattering objects within the propagation environment, and under the coverage of both receiving and transmitting antennas [1] [3]. In this case, the scattering objects are assumed to lie along the ellipse, and the MS1 and MS2 are placed at the foci of the ellipse, as shown in the figure 1.2.

The Space-Time Correlation properties cover the influence of details such as the spatial angles for Angles of Arrival, Angles of Departure, the geometry of the antenna arrays at the MS1 and MS2, the distances between the MS1 and MS2, and relative distances from the scatterers located along the ellipse, the MS speed vector (direction and speed of travel of the MS), the wave propagation velocity, position of the p^{th} antenna on the MS1 side relative to the MS1 coordinates, position of the q^{th} antenna on the MS2 side relative to the MS2 coordinates, Time delay between p^{th} MS1 and the q^{th} MS2 antenna, and the number of total dominant paths.

2.3.3 Space Doppler (SD) Power Spectral Density (PSD)

Due to Doppler Effect, if a transmitter is moving away from a receiver, the frequency of the received signal is lower than the one sent out from the transmitter; otherwise, the frequency is increased. In wireless communications, there are many factors that can cause relative movement between a transmitter and a receiver. It can be the movement of a mobile or it can be the movement of some objects in the background that causes the change of path length between the transmitter and the receiver. The lengths of signal path are often different, which

correspond to different movement speeds of transmitter signals, and in turn different frequency shifts on the signal paths. As a result, a frequency spread is caused in the signal spectrum.

The energy spectral density describes how the energy (or variance) of a signal is distributed with frequency.

2.3.4 Level Crossing Rate (LCR)

The Level Crossing Rate and Average Fading Duration are two important second order statistics that make the Mobile-to-Mobile channels significantly different from Fixed-to-Mobile (F2M) channels.

The Level Crossing Rate is a measure of the rapidity of the fading. It quantifies how often the fading crosses some threshold, usually in the positive-going direction.

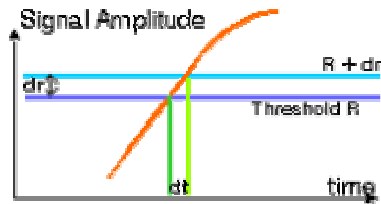


Figure 2.2 Level Crossing Rate (LCR) threshold.

The figure 2.2 show the crossing of the threshold R with width dr lasts for dt seconds. The derivative of the signal amplitude, with respect to time, is dr / dt .

If the signal always crosses the threshold with the same derivative, then:

Average number of crossings per second * dt = Probability that the amplitude is in the interval $[R, R + dr]$.

Therefore, the probability that the signal amplitude is within the window $[R, R + dr]$ is known from the probability density of the signal amplitude.

Moreover, the joint PDF of signal amplitude and its derivative can be found.

2.3.5 Average Fade Duration (AFD)

The average fade duration quantifies how long the signal spends below the threshold.

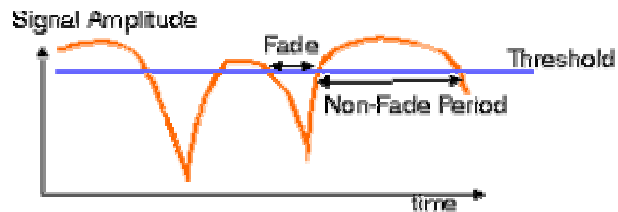


Figure 2.3 AFD fade and non-fade periods for a sample of a fading signal.

As the amplitude of a signal received over such a channel also fluctuates, the receiver will experience periods during which the signal can not be recovered reliably. If a certain minimum (threshold) signal level is needed for acceptable communication performance, the received signal will experience periods of:

- Sufficient signal strength or "non-fade intervals", during which the receiver can work reliably and at low bit error rate.
- Insufficient signal strength or "fades", during which the bit error rate inevitably is close to one half (randomly guessing ones and zeros) and the receiver may even fall out of lock.

Channel fading occurs mainly because the user moves. If the user is stationary almost no time variations of the channel occur (except if reflecting elements in the environment move).

The AFD is inversely proportional to the speed of the mobile user.

The fade durations rapidly reduce with increasing fade margin, but the time between fades increases much slower.

3 A Mathematical representation of the MIMO M2M Geometric Elliptical Model

3.1 Determining the MIMO M2M Elliptical Model properties

The Elliptical Scattering Model describes a system where the two mobile stations MS1 and MS2 are located at the focal points of the ellipse, these mobile stations are described as a vectors, each with magnitude (speed V_T and V_R) and direction (angles of motion γ_T and γ_R).

The circumference of the ellipse describe all the local effective scatterers $S_{TR}^{(n)}$ associated with the Angles of Departure of the waves bounced and designated by $\phi_T^{(n)}$, this waves travel the distance defined by the $\xi_T^{(n)} + \xi_R^{(n)} = 2a$.

The major axis is denoted by 'a' and the minor axis of the ellipse is the denoted by 'b'.

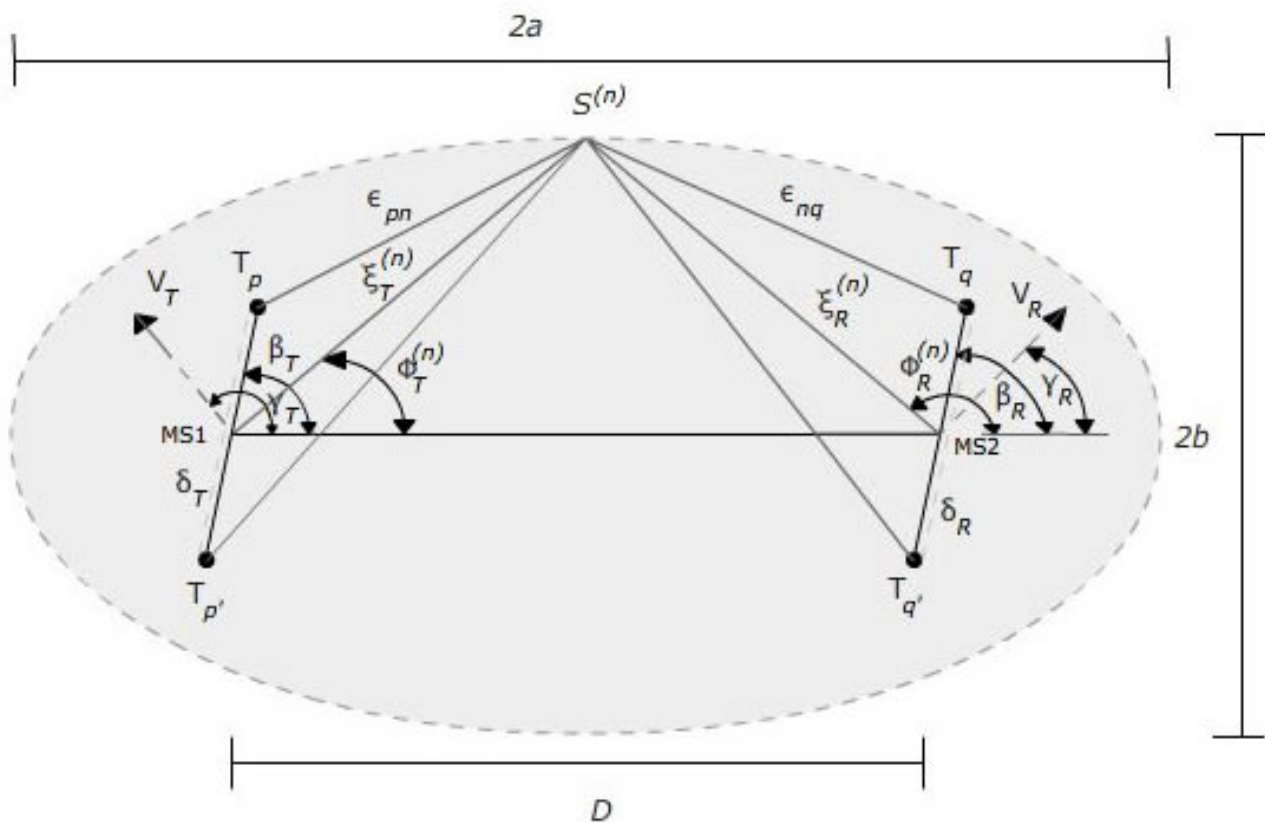


Figure 3.1 Geometric Elliptical Scattering model for a MIMO M2M channel with local scatterers $S(n)$ lying on an ellipse.

Here, we assume that both the MS1 and MS2 are able to receive and transmit information. In this case the MS1 will be the transmitter and MS2 will be the receiver, these two stations are equipped with a uniform linear antenna array consisting of MT and MR antenna elements respectively.

The angles shown in the figure 3.1 represent the tilt angles of the Transmit (β_T) and Receive (β_R) antenna arrays, the Angle of Departure and the Angle of Arrival. The antenna element distance (spacing) δ_T at Tx and δ_R at Rx.

3.2 The MIMO M2M Elliptical Reference Model

One important relationship between the MS1 and MS2 is the assumption that the number of local scatterers is infinite. Therefore, the diffuse component at each of the receive antennas is composed of an infinite number of homogeneous plane waves.

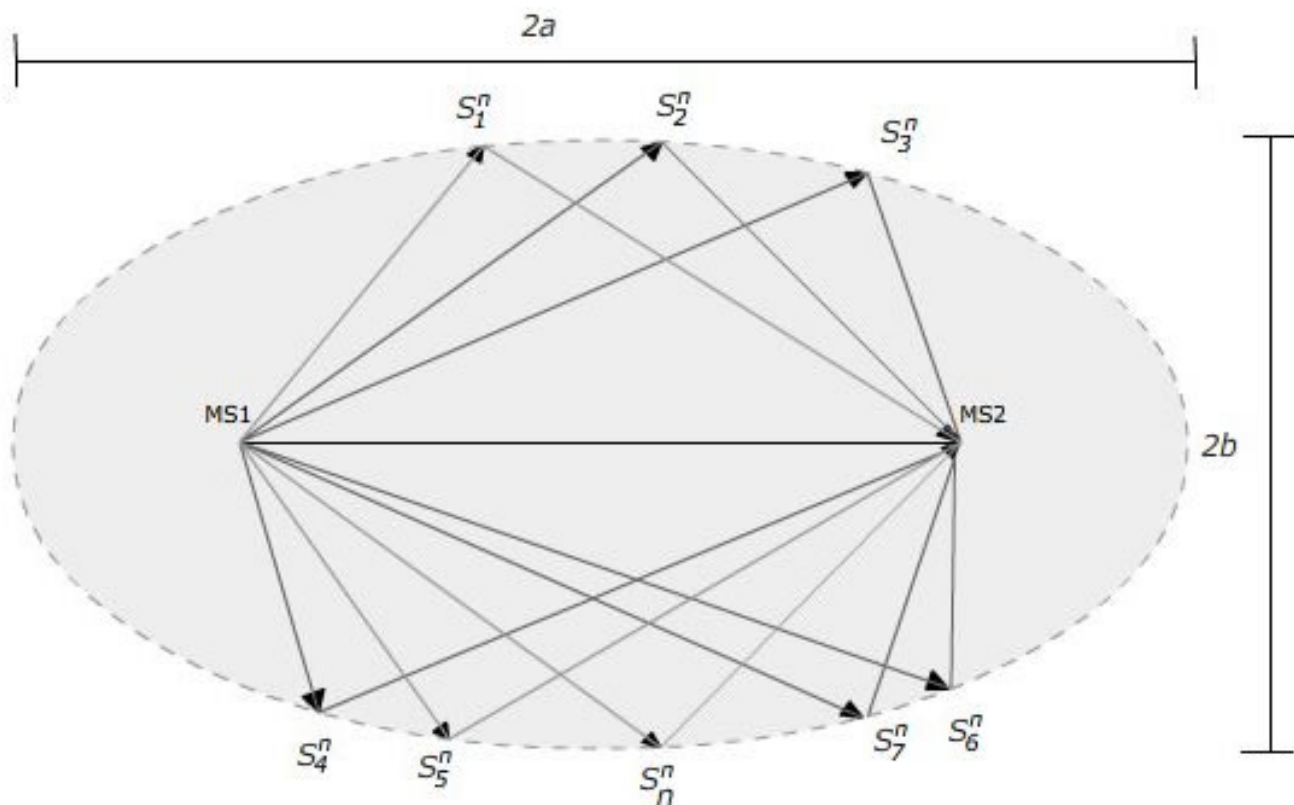


Figure 3.2 Geometric Elliptical Scattering model for a Wideband MIMO M2M channel with Multiple Clusters of scatterers $S(n)$ lying on an ellipse.

The figure 3.2 show the points where the scatterers lye along the Ellipse and the path taken by the signal within the MIMO M2M channel.

An important property of the Ellipse is that the sum of the distances from any point on the curve to the focal points is constant, therefore we can mathematically define the impulse response of the Ellipse.

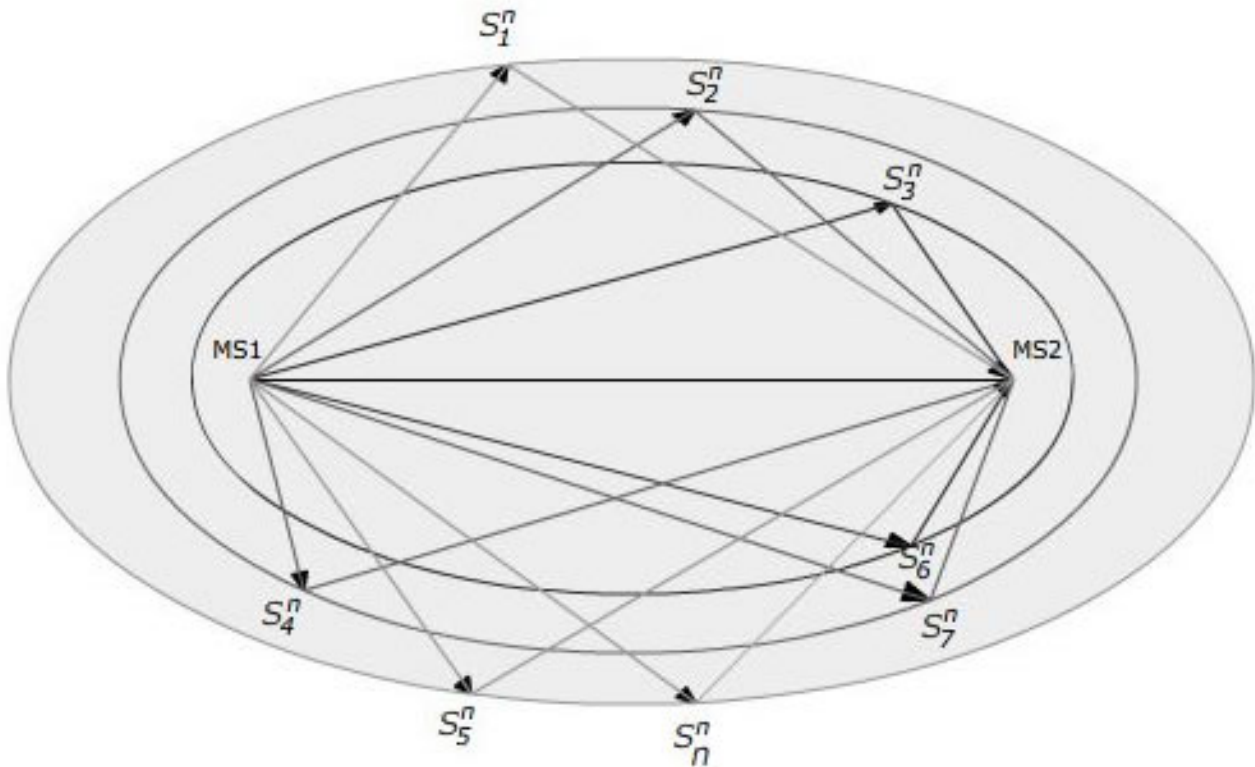


Figure 3.3 Geometric Elliptical Scattering model for a Wideband MIMO M2M channel with Multiple Clusters of scatterers $S(n)$ lying on L ellipses.

In the figure 3.3 the MS1 and MS2 are surrounded by multiple ellipses which represent the different propagation paths with their corresponding propagation delays.

From this reference model, applying the multiple elliptical layers to the Tapped Delay line model shown in figure 3.4, where each ellipse is represented by a Tap and then perform a study on the frequency correlation properties of the different ellipses.

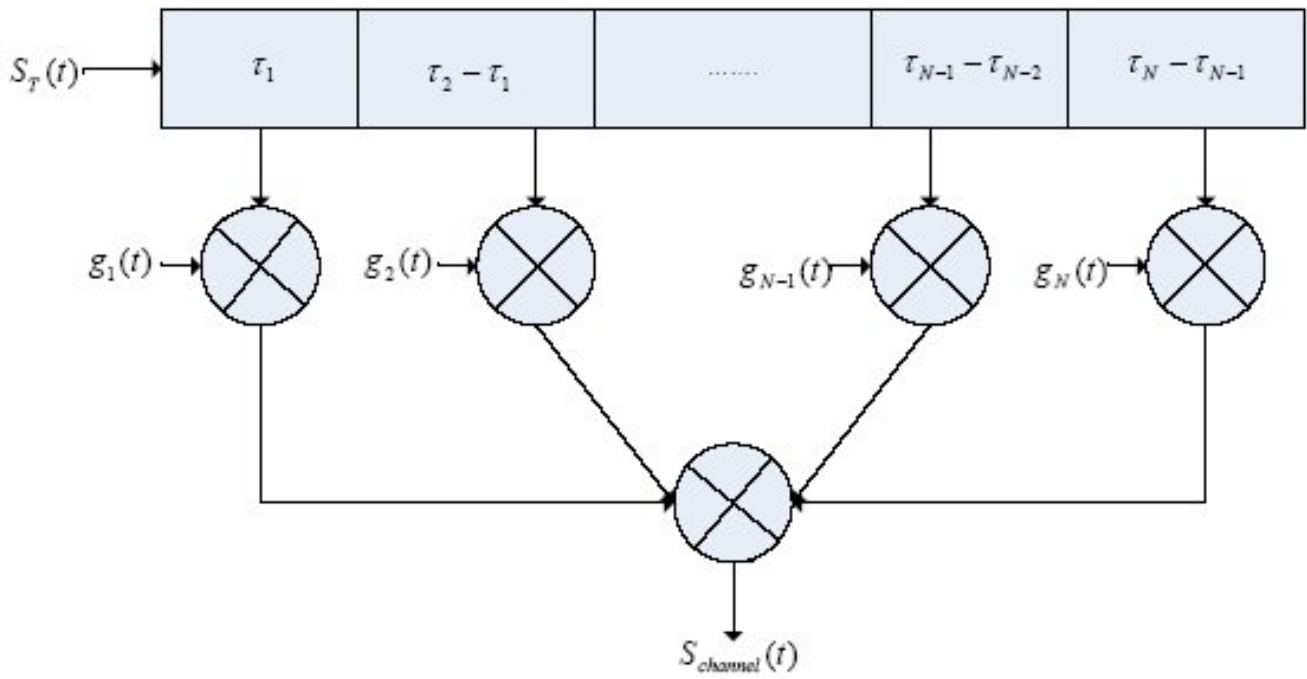


Figure 3.4 A Tapped Delay line model for discrete multipath channels.

3.3 MIMO M2M Mathematical Representation

A few assumptions were made while resolving these equations and they are stated as we proceed.

The received signal is constructed as a sum of the Line of Sight and Single Bounced rays with different energies.

- Generic and adaptive geometrical-based stochastic reference model for Space Time (ST) correlated MIMO M2M Ricean fading channels.
- From the model, the ST Correlation Function (CF) and the corresponding Space-Doppler (SD) Power Spectral Density (PSD), Level Crossing Rate (LCR) and Average Fade Duration (AFD) are derived for a 2D non-isotropic scattering environment.

Consider in this MIMO M2M Elliptical ring model with Single Bounced rays the distance (D) between the Tx and Rx, the number of effective scatterers (N) lie on an ellipse with Tx and Rx located at the foci.

The semimajor axis of the ellipse and the n^{th} ($n = 1, \dots, N$) effective scatterer are denoted by a and $S_{TR}^{(n)}$.

The antenna element spacing δ_T at Tx and δ_R at Rx.

Multi-element antenna tilt angles are β_T and β_R .

The Tx and Rx move with speed V_T and V_R in directions determined by the angles of motion γ_T and γ_R .

ϕ_{Rq}^{LoS} denotes the AoA of a LoS path.

The AoA of the waves traveling from the effective scatterers $S_{TR}^{(n)}$ towards the Rx are denoted by $\phi_R^{(n)}$.

The AoDs of the waves that impinge on the effective scatterers $S_{TR}^{(n)}$ are designated by $\phi_T^{(n)}$.

The received complex impulse response for $T_p - R_q$ link is a superposition of the LoS and Single Bounced rays.

$$h_{pq}(t) = h_{pq}^{LoS}(t) + h_{pq}^{EL}(t) \quad (1)$$

$$h_{pq}^{LoS}(t) = \sqrt{\frac{K_{pq}\Omega_{pq}}{K_{pq}+1}} e^{-j2\pi f_c \tau_{pq}} \times e^{j[2\pi f_{T\max} t \cos(\pi - \phi_{Rq}^{LoS} + \gamma_T) + 2\pi f_{R\max} t \cos(\phi_{Rq}^{LoS} + \gamma_R)]} \quad (2)$$

$$h_{pq}^{EL}(t) = \sqrt{\frac{\Omega_{pq}}{K_{pq}+1}} \lim_{N \rightarrow 0} \sum_{n=1}^N \frac{1}{\sqrt{N}} e^{j(\psi_n - 2\pi f_c \tau_{pq,n})} \quad (3)$$

where $p = 1, 2, \dots, M_T$ and $q = 1, 2, \dots, M_R$

The Time delay between the p^{th} MS1 and q^{th} MS2 antenna elements as described in the elliptical figure 3.1 can be deduced by dividing the distances by the speed of light, c , the wave propagation velocity $\tau_{pq} = \frac{\mathcal{E}_{pq}}{c}$.

The travel times of the waves through the link $T_p - R_q$

$$\tau_{pq,n} = \frac{(\mathcal{E}_{pn} + \mathcal{E}_{nq})}{c} \quad (4)$$

where c is the speed of light, K_{pq} is the Ricean factor of $T_p - R_q$ link, Ω_{pq} is the total power transferred through $T_p - R_q$ link, the Maximum Doppler frequencies associated with the Tx

$$f_{T\max} \rightarrow \frac{V_T}{\lambda} \text{ and } f_{R\max} \rightarrow \frac{V_R}{\lambda}.$$

The distances between the Transmitter and the Receiver antennas to the scatterers along the ellipse, can be expressed in terms of the antenna element spacing, the Angle of Arrival and the Angle of Departure. Distances \mathcal{E}_{pq} can be expressed as functions of the relevant angles.

Assuming $D \gg \{\delta_T, \delta_R\}$ and using the laws of cosines and sines, the distances can be calculated as follows.

For the Line of Sight (LoS)

$$\mathcal{E}_{pq} \approx \mathcal{E} - K_q \delta_R \cos(\phi_{Rq}^{LoS} - \beta_R) \quad (5)$$

$$\mathcal{E} \approx D - K_q \delta_T \cos \beta_T \quad (6)$$

For macro and micro-cell scenarios where $D \gg \max\{R_T, R_R\}$

$$\phi_{Rq}^{LoS} \approx \pi \quad (7)$$

For pico-cell scenarios where $D \gg \max\{R_T, R_R\}$ is not fulfilled

$$\phi_{Rq}^{LoS} \approx \pi - \frac{K_p \delta_T \sin \beta_T}{D} \quad (8)$$

$$K_p = \frac{(M_T - 2p + 1)}{2} \quad (9)$$

$$K_q = \frac{(M_R - 2q + 1)}{2} \quad (10)$$

For the Single-bounced component of the Elliptical-ring model

$$\varepsilon_{pn} \approx \xi_T^n - K_p \delta_T \cos(\phi_T^{(n)} - \beta_T) \quad (11)$$

$$\varepsilon_{nq} \approx \xi_R^n - K_q \delta_R \cos(\phi_R^{(n)} - \beta_R) \quad (12)$$

where

$$\xi_T^{(n)} = \frac{a^2 + \frac{D^2}{4} + aD \cos \phi_R^{(n)}}{a + \frac{D \cos \phi_R^{(n)}}{2}} \quad (13)$$

$$\xi_R^{(n)} = \frac{b^2}{a + \frac{D \cos \phi_R^{(n)}}{2}} \quad (14)$$

In order to reduce the computational complexity we use a new exact and simple relationship between the AoA and AoD for the MIMO M2M Elliptical ring model to replace the previous approximate relationship in [10]. Consider $f = D/2$, based on the application of the law of cosines and sines in the triangle $O_T S_T^{(n)} O_R$ from figure 3.1, we obtain

$$\left(\xi_T^{(n)}\right)^2 = \left(\xi_R^{(n)}\right)^2 + 4f^2 + 4f \xi_R^{(n)} \cos \phi_R^{(n)} \text{ and } \left(\xi_T^{(n)}\right) / \sin \phi_R^{(n)} = \left(\xi_R^{(n)}\right) / \sin \phi_T^{(n)}, \text{ respectively.}$$

Using $\xi_T^{(n)} + \xi_R^{(n)} = 2a$, the exact relationship between the AoA and AoD as

$$\sin \phi_T^{(n)} = \frac{b^2 \sin \phi_R^{(n)}}{a^2 + f^2 + 2af \cos \phi_R^{(n)}} \quad (15)$$

$$\cos \phi_T^{(n)} = \frac{2af + (a^2 + f^2) \cos \phi_R^{(n)}}{a^2 + f^2 + 2af \cos \phi_R^{(n)}} \quad (16)$$

In order to characterize the AoD $\phi_T^{(n_i)}$ and AoA $\phi_R^{(n_i)}$, we use the von Mises PDF defined as $f(\phi) \triangleq \exp[k \cos(\phi - \mu)] / 2\pi I_0(k)$, where $\phi \in [-\pi, \pi]$, $I_0(\cdot)$ is the zero order modified Bessel function of the first kind, $\mu \in [-\pi, \pi]$ accounts for the mean value of the angle ϕ , and $k (k \geq 0)$ is a real valued parameter that controls the angle spread of the angle ϕ [11].

3.3.1 ST CF and SD PSD

We can derive the equations for the MIMO M2M Elliptical model statistical properties, Space Time, Correlation Function and Space-Doppler Power Spectral Density.

Based on the proposed channel model we will derive the ST CF and the corresponding SD PSD for 2D non-isotropic scattering environment.

3.3.1.1 ST CF

The normalized ST CF between any two complex impulse responses $h_{pq}(t)$ and $h_{p'q'}^\dagger(t)$ is defined as

$$\rho_{h_{pq}h_{p'q'}}(\tau) = \frac{E[h_{pq}(t)h_{p'q'}^\dagger(t+\tau)^*]}{\sqrt{E[|h_{pq}(t)|^2]E[|h_{p'q'}(t)|^2]}} \quad (17)$$

where $(\cdot)^*$ denotes the complex conjugate operation, $E[\cdot]$ is the statistical expectation operator, $p, p' \in \{1, 2, \dots, M_T\}$ and $q, q' \in \{1, 2, \dots, M_R\}$. This is a function of time separation τ and antenna elements spacing δ_T and δ_R .

Using trigonometric transformations $\int_{-\pi}^{\pi} \exp(a \times \sin c + b \cos c) = 2\pi I_0(\sqrt{a^2 + b^2})$

In the case of LoS component,

$$\rho_{h_{pq}^{LoS}h_{p'q'}^{LoS}}(\tau) = \sqrt{K_{pq}K_{p'q'}} e^{j2\pi G - j2\pi\tau H} \quad (18)$$

Where for macro – micro – cell scenarios

$$G = P \cos \beta_T - Q \cos \beta_R \quad (19)$$

$$H = f_{T_{\max}} \cos \gamma_T - f_{R_{\max}} \cos \gamma_R \quad (20)$$

and for pico – cell scenarios

$$G = P \cos \beta_T - Q \cos \beta_R + \frac{\sin \beta_T \sin \beta_R (P(M_R + 1)\delta_R + Q(M_T + 1)\delta_T - 2U)}{2D} \quad (21)$$

$$H = f_{T\max} \left(\cos \gamma_T + \frac{K_{p'} \delta_T \sin \beta_T \sin \gamma_T}{D} \right) - f_{R\max} \left(K_{p'} \delta_T \times \sin \beta_T \sin \gamma_R - \frac{\cos \gamma_R}{D} \right) \quad (22)$$

$$P = (p' - p) \delta_T / \lambda \quad (23)$$

$$Q = (q' - q) \delta_R / \lambda \quad (24)$$

$$U = (p'q' - pq) \delta_T \delta_R / \lambda \quad (25)$$

$$K_{p'} = (M_T - 2p' + 1) / 2 \quad (26)$$

$$K_{q'} = (M_R - 2q' + 1) / 2 \quad (27)$$

The single bounced component of the elliptical-ring model.

$$\rho_{h_{pq}^{EL} h_{p'q'}^{EL}}(\tau) = \frac{n_{SB}}{2\pi I_0(K_R^{SB})} \int_{-\pi}^{\pi} e^{J + j2\pi(T - \tau V)} \quad (28)$$

non-isotropic

$$J = K_R^{SB} \cos(\phi_R^{SB} - \mu_R^{SB}) \quad (29)$$

Space

$$T = P \cos(\phi_T^{SB} - \beta_T) + Q \cos(\phi_R^{SB} - \beta_R) \quad (30)$$

Time

$$V = f_{T\max} \cos(\phi_T^{SB} - \gamma_T) + f_{R\max} \cos(\phi_R^{SB} - \gamma_R) \quad (31)$$

where

μ_R^{SB} is the mean value of AoA ϕ_R^{SB} .

K_R^{SB} controls the angle spread of the AoA ϕ_R^{SB} .

3.3.1.2 SD PSD

Applying the Fourier transformation in terms of time to the ST CF, we obtain

$$F \left\{ \rho_{h_{pq}h_{p'q'}}(\tau) \right\} = \int_{-\infty}^{\infty} \rho_{h_{pq}h_{p'q'}}(\tau) e^{-j2\pi f_D \tau} d\tau \quad (32)$$

where f_D is the Doppler frequency.

In the case of the LoS components

$$F \left\{ \rho_{h_{pq}^{LoS}h_{p'q'}^{LoS}}(\tau) \right\} = \sqrt{K_{pq}K_{p'q'}} e^{j2\pi G} \delta(f_D + H) \quad \text{where } \delta(\cdot) \text{ denotes the Dirac delta function.}$$

In the case of single bounced component of the elliptical-ring model we must evaluate the integral in (32).

3.3.2 LCR and AFD

Based on the introduced channel model, I will derive the LCR and AFD for a non-isotropic scattering environment. First need to be defined the appropriate time autocorrelation function (ACF) and the notion of spectral moments, which are fundamentals of further deriving the LCR and AFD in this section. The ACF of the complex impulse response of diffuse component $h_{pq}^{DIF}(t)$ is defined as $\rho_{h_{pq}^{DIF}}(\tau) = E[h_{pq}^{DIF}(t)h_{pq}^{DIF*}(t+\tau)]$, where $(\cdot)^*$ denotes the complex conjugate operation, $E[\cdot]$ is the statistical expectation operator. It is shown in (5) that based on the application of the von Mises PDF and trigonometric transformations, the time ACF of single bounced components are given by

$$\rho_{h_{pq}^{EL}}(\tau) = \frac{n_{SB}\Omega_{pq}}{2\pi(K_{pq}+1)I_0(K_R^{SB})} \int_{-\pi}^{\pi} e^{J-j2\pi\tau V} d\phi_R^{SB} \quad (33)$$

where $J = k_R^{SB} \cos(\phi_R^{SB} - \mu_R^{SB})$, $V = f_{T\max} \cos(\phi_T^{SB} - \gamma_T) + f_{R\max} \cos(\phi_R^{SB} - \gamma_R)$, with ϕ_T^{SB} (ϕ_R^{SB}) being the continuous notations of $\phi_T^{(n)}$ ($\phi_R^{(n)}$).

The n^{th} spectral moment, b_n ($n = 0, 1, 2, \dots$), is defined to be $b_n = \left. \frac{d^n \rho_{pq}^{DIF}(\tau)}{2j^n d\tau^n} \right|_{\tau=0}$, where $j^2 = -1$.

Based on the application of the von Mises PDF, the spectral moments b_1^{SB} and b_2^{SB} for the single bounced component can be derived by successive differentiation of

$$b_1^{SB} = -b_0^{SB} \int_{-\pi}^{\pi} \frac{e^{kR \cos(\phi_R^{SB} - \mu_R)} L_R}{I_0(k_R)} d\phi_R^{SB} \quad (34)$$

$$b_2^{SB} = b_0^{SB} \int_{-\pi}^{\pi} \frac{2\pi e^{kR \cos(\phi_R^{SB} - \mu_R)} L_R^2}{I_0(k_R)} d\phi_R^{SB} \quad (35)$$

where $L_R = f_{T \max} \cos(\phi_T^{SB} - \gamma_T) + f_{R \max} \cos(\phi_R^{SB} - \gamma_R)$, $b_0^{SB} = \frac{n_{SB} \Omega_{pq}}{2(K_{pq} + 1)}$.

For a fading signal, the LCR $N_R(r_n)$, is by definition the average number of times per second that the single envelope, $R(t) = |h_{pq}(t)|$, crosses a specified level r_n with positive/negative slope.

The AFD, $T_R-(r_n)$, is the average time over which the signal envelope, $R(t)$, remains below certain level r_n . In general, the AFD $T_R-(r_n)$ is defined by [11].

$$T_R-(r_n) = \frac{P_R-(r_n)}{N_R(r_n)} \quad (36)$$

where $P_R-(r_n) = 1 - Q\left(\sqrt{2K_{pq}} \sqrt{2(K_{pq} + 1)r_n}\right)$ indicates a cumulative distribution function of $R(t)$ with $Q(\cdot, \cdot)$ denoting the generalized Marcum Q function.

4 Results and analysis of the MIMO M2M Statistical Properties

4.1 Space Doppler frequency Power Spectral Density

In this section I will present the numerical results of the Doppler PSD for elliptical ring model with single bounced.

The spectral shape of the Doppler spread determines the time domain fading waveform and dictates the temporal correlation and fade slope behaviors.

4.1.1 SD PSD in isotropic scattering environment

For this first simulation consider an isotropic scattering environment.

The parameters used for this numerical analysis:

$$f_c = 5.9\text{GHz}, f_{T_{\max}} = f_{R_{\max}} = 570\text{Hz}, \beta_T = \pi/3, \beta_R = \pi/4, a = 250\text{m}, D = 350\text{m}$$

$$\gamma_T = 0, \gamma_R = \pi, K_T = 0, K_R = 0, \mu_T = 0, \mu_R = \pi, K_{pq} = 5$$

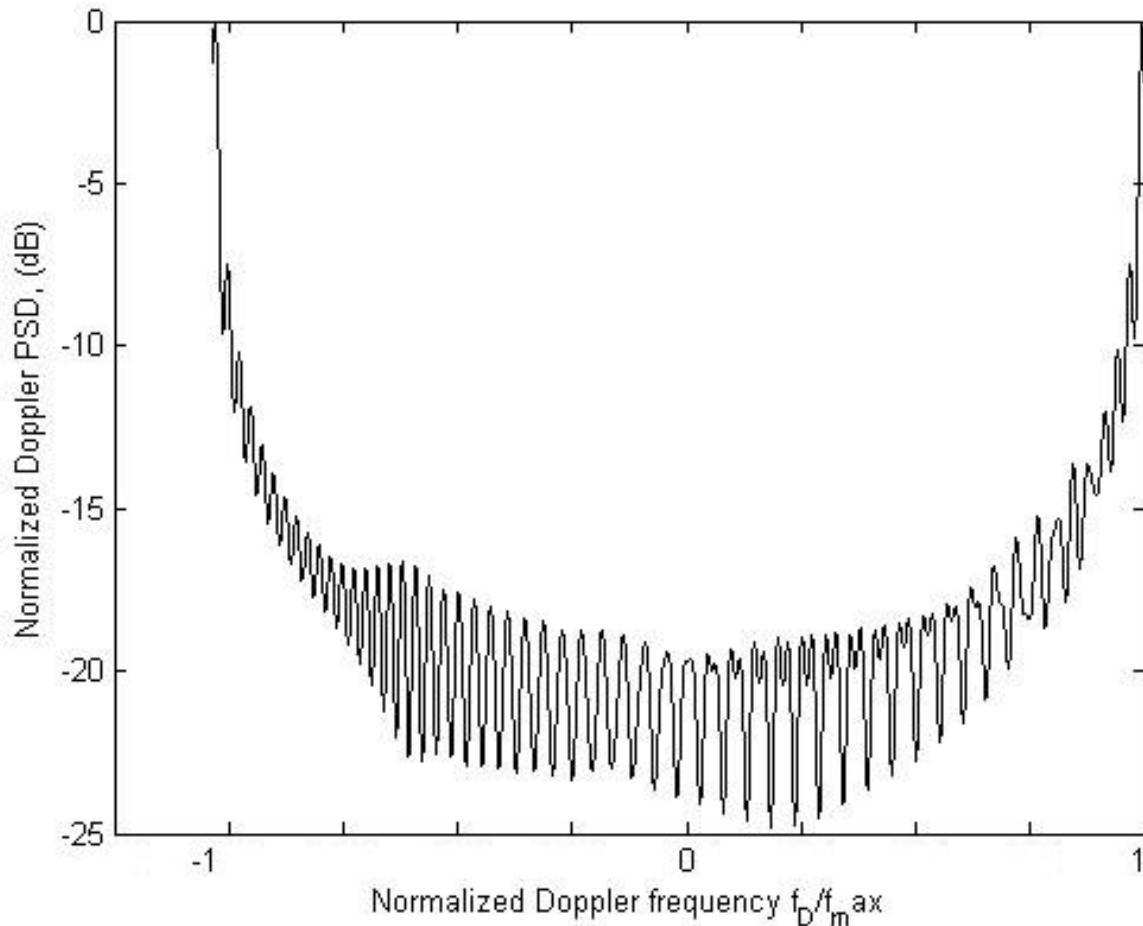


Figure 4.1.1 SD PSD $k_T = k_R = 0$ isotropic scattering environment.

This figure describes two mobile stations moving in opposite direction determined by the angle of direction ($\gamma_T = 0, \gamma_R = \pi$). The $k_T = k_R = 0$ means that the environment is an isotropic scattering environment, this parameter controls the angle spread. The result is a Power Spectral Density similar to the U shape with small variations.

4.1.2 SD PSD in non isotropic scattering environment

Considering the same parameters as the figure 4.1.1, except that in this case is a non isotropic scattering environment.

The parameters used for this numerical analysis:

$$f_c = 5.9\text{GHz}, f_{T\max} = f_{R\max} = 570\text{Hz}, \beta_T = \pi / 3, \beta_R = \pi / 4, a = 250\text{m}, D = 350\text{m}$$

$$\gamma_T = 0, \gamma_R = \pi, K_T = 1, K_R = 1, \mu_T = 0, \mu_R = \pi, K_{pq} = 5$$

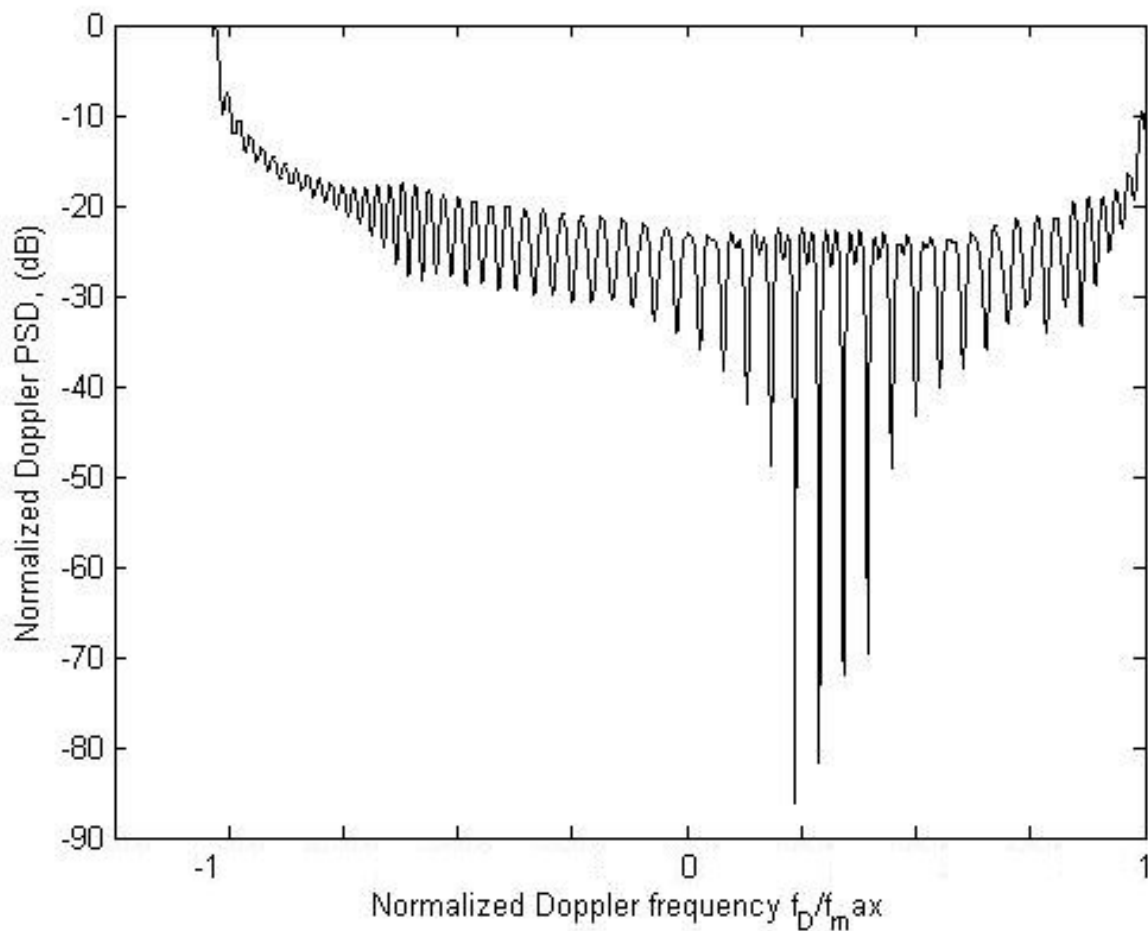


Figure 4.1.2 SD PSD $k_T = k_R = 1, \gamma_T = 0, \gamma_R = \pi$, non isotropic moving in opposite directions.

This figure describes two mobile stations moving in opposite direction determined by the angle of direction ($\gamma_T = 0, \gamma_R = \pi$) in a non isotropic scattering environment ($k_T = k_R = 1$), the mean value of the angle determined by $\mu_T = 0, \mu_R = \pi$. The result is a Power Spectral Density similar to the *U* shape obtained in the isotropic scattering environment. Nevertheless this PSD is translated to the positive values and the plot contains notorious changes concluding that the mean angle value affects the received signal causing random modulations.

4.1.3 SD PSD moving in the same directions

For this numerical analysis, in a non isotropic scattering environment moving in the same direction, the parameters: $\gamma_T = 0, \gamma_R = 0, K_T = 1, K_R = 1, \mu_T = 0, \mu_R = \pi, K_{pq} = 5$

$$f_c = 5.9\text{GHz}, f_{T\max} = f_{R\max} = 570\text{Hz}, \beta_T = \pi/3, \beta_R = \pi/4, a = 250\text{m}, D = 350\text{m}$$

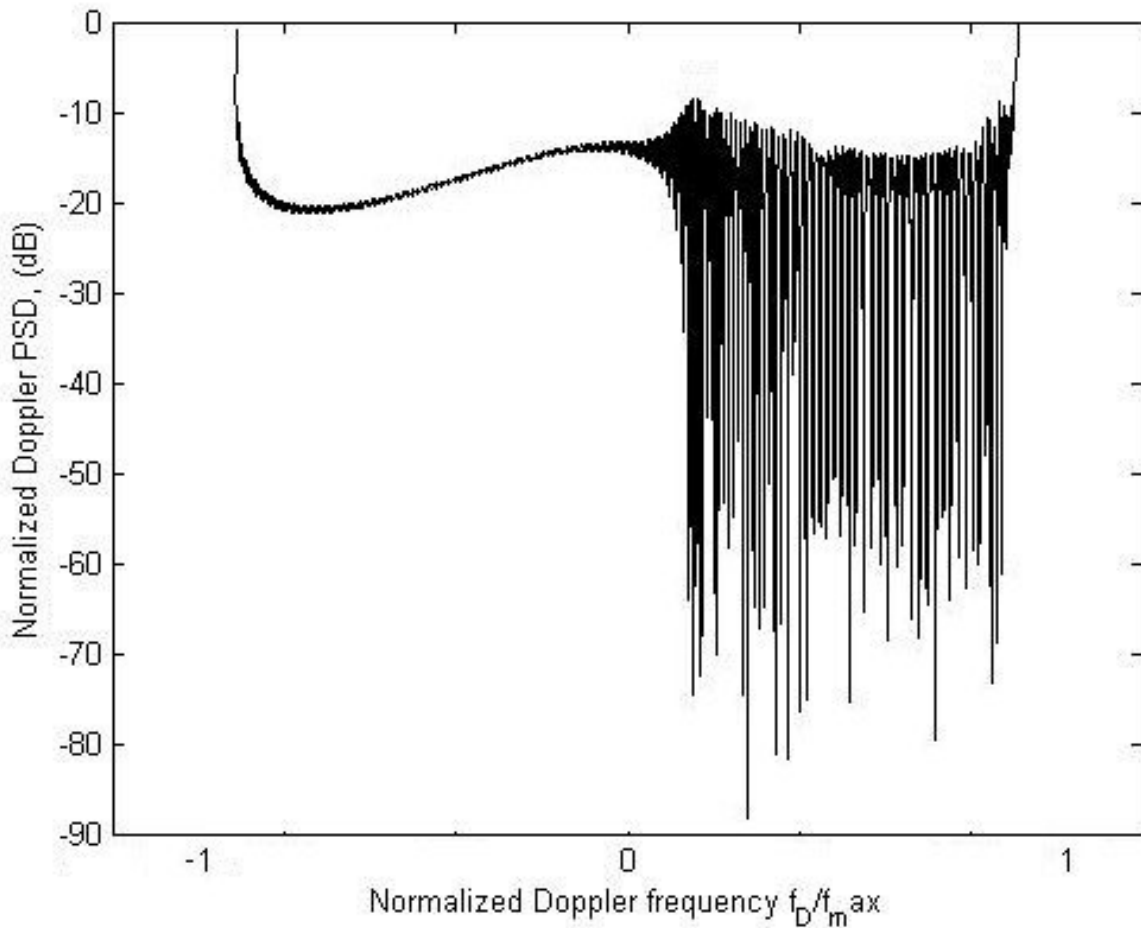


Figure 4.1.3 SD PSD $k_T = k_R = 1, \gamma_T = 0, \gamma_R = 0$, non isotropic moving in the same directions.

This figure describes two mobile stations moving in the same direction determined by the angle of direction ($\gamma_T = 0, \gamma_R = 0$) in a non isotropic scattering environment ($k_T = k_R = 1$), the mean value of the angle determined by $\mu_T = 0, \mu_R = \pi$. In this case were the two mobile stations move in the same direction, the minimum Doppler shift occurs for a wave coming from the same direction the antenna is moving to.

4.1.4 SD PSD moving in opposite directions

The parameters used for this numerical analysis:

$$f_c = 5.9\text{GHz}, f_{T\max} = f_{R\max} = 570\text{Hz}, \beta_T = \pi/3, \beta_R = \pi/4, a = 250\text{m}, D = 350\text{m}$$

$$\gamma_T = 0, \gamma_R = \pi, K_T = 3, K_R = 3, \mu_T = 0, \mu_R = \pi, K_{pq} = 5$$

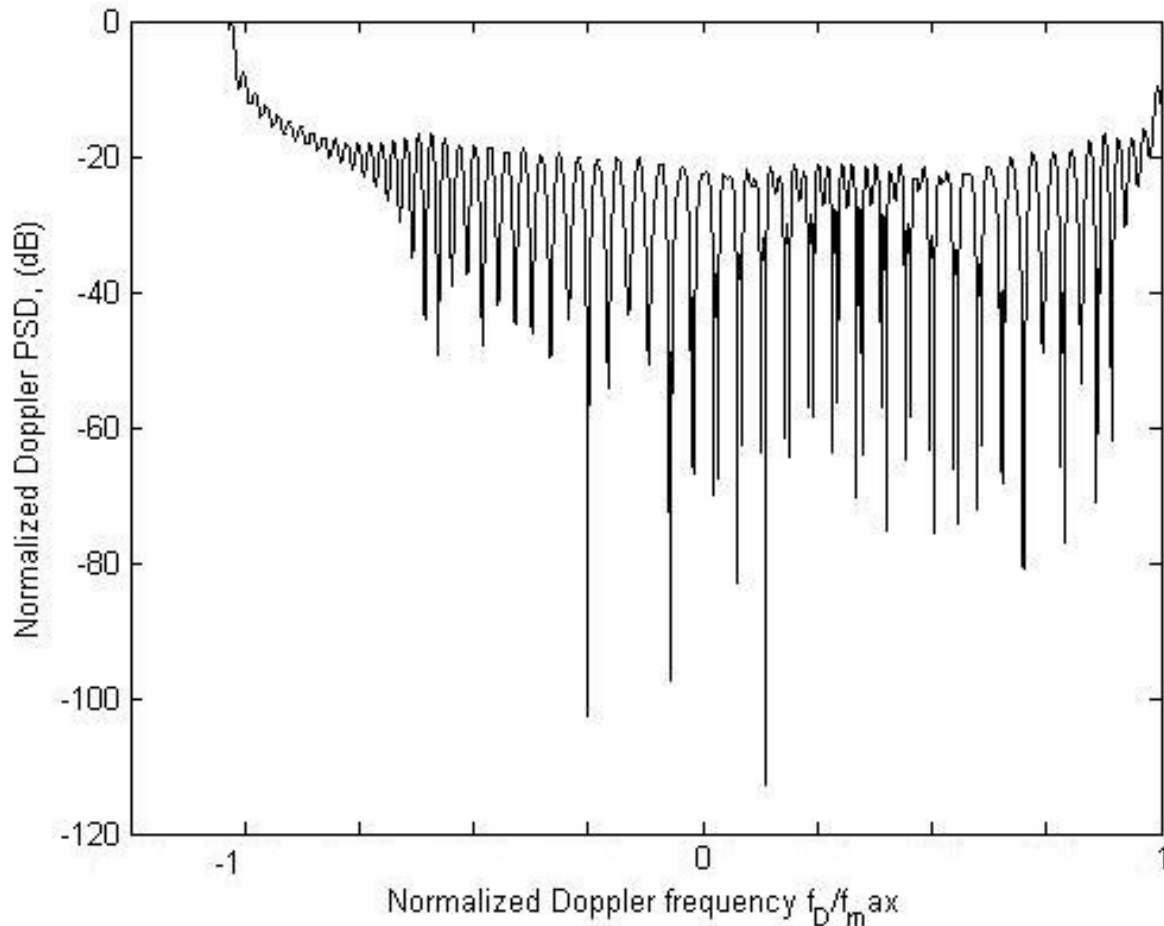


Figure 4.1.4 SD PSD $k_T = k_R = 3, \gamma_T = 0, \gamma_R = \pi$, non isotropic moving in opposite directions.

This figure describes two mobile stations moving in the opposite direction determined by the angle of direction ($\gamma_T = 0, \gamma_R = \pi$) in a non isotropic scattering environment ($k_T = k_R = 3$), the mean value of the angle determined by $\mu_T = 0, \mu_R = \pi$. The result is a Power Spectral Density similar to a *U* shape with more uniform multiple changes over the spectrum, the maximum Doppler shift occurs for a wave coming from the opposite direction as the direction the antenna is moving to.

It is clear that the shape of the Doppler PSD for the elliptical ring model with single bounced rays is similar to the *U* shape. Considering the results of the numerical analysis, no matter what the propagation environment is, for M2M channels in non isotropic scattering environments, the single bounced rays will cause a Doppler PSD similar to the *U* shape.

4.2 Level Crossing Rate and Average Fading Duration

The next numerical analysis for LCR and AFD of the MIMO M2M model consider different angle spreads, mean angles, and directions of motion ($K_{pq} = 0$);

same direction ($\gamma_T = \gamma_R = 0$);

opposite direction ($\gamma_T = 0, \gamma_R = \pi$);

Based on the derived LCR and AFD in section 3, the two second order statistics of the non-isotropic MIMO M2M Ricean fading channel are numerically analyzed in more detail in terms of some important parameters.

The following parameters were used for the numerical analysis:

$$f_c = 5.9GHz, f_{T_{\max}} = f_{R_{\max}} = 570Hz, \beta_T = \pi / 3, \beta_R = \pi / 4, a = 400m, D = 600m$$

$$\gamma_T = 0, \gamma_R = \pi, K_T = 0, K_R = 0, \mu_T = 0, \mu_R = \pi, K_{pq} = 5$$

For isotropic scattering environments ($k_T = k_R = 0$), the LCR and AFD change according to the different directions of motion. In non-isotropic scattering environments the Elliptical model with single-bounced rays to the LCR and AFD are completely different for M2M channels.

In the next figures can be observed that the angle spreads (related to the values of k_T and k_R), mean angled (related to the values of μ_T and μ_R), and directions of motion (related to the values of γ_T and γ_R) significantly affect the LCR and AFD. Therefore, for non-isotropic scattering environments these parameters play an important role affecting the behavior of the LCR and AFD.

4.2.1 LCR and AFD $k_T = k_R = 0$ isotropic scattering environment

The parameters used for this numerical analysis:

$$f_c = 5.9\text{GHz}, f_{T\text{max}} = f_{R\text{max}} = 570\text{Hz}, \beta_T = \pi / 3, \beta_R = \pi / 4, a = 400\text{m}, D = 600\text{m}$$

$$\gamma_T = 0, \gamma_R = \pi, \mu_T = 0, \mu_R = \pi, K_{pq} = 5$$

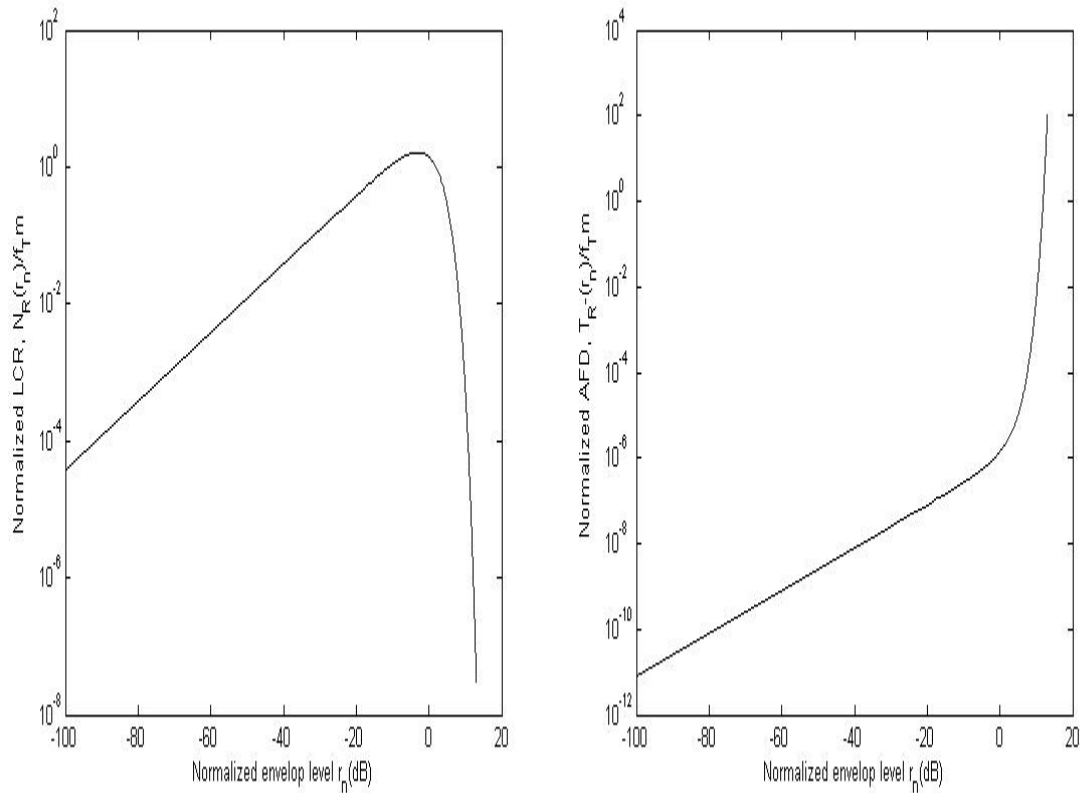


Figure 4.2.1 LCR and AFD $k_T = k_R = 0$ isotropic scattering environment.

The LCR curve has a maximum if the local-mean-power is about as large as the threshold noise or interference power.

4.2.2 LCR and AFD $k_T = k_R = 3, \mu_T = 0, \mu_R = \pi$ non isotropic environment

The parameters used for this numerical analysis:

$$f_c = 5.9\text{GHz}, f_{T_{\max}} = f_{R_{\max}} = 570\text{Hz}, \beta_T = \pi / 3, \beta_R = \pi / 4, a = 400\text{m}, D = 600\text{m}$$

$$\gamma_T = 0, \gamma_R = \pi, \mu_T = 0, \mu_R = \pi, K_{pq} = 5$$

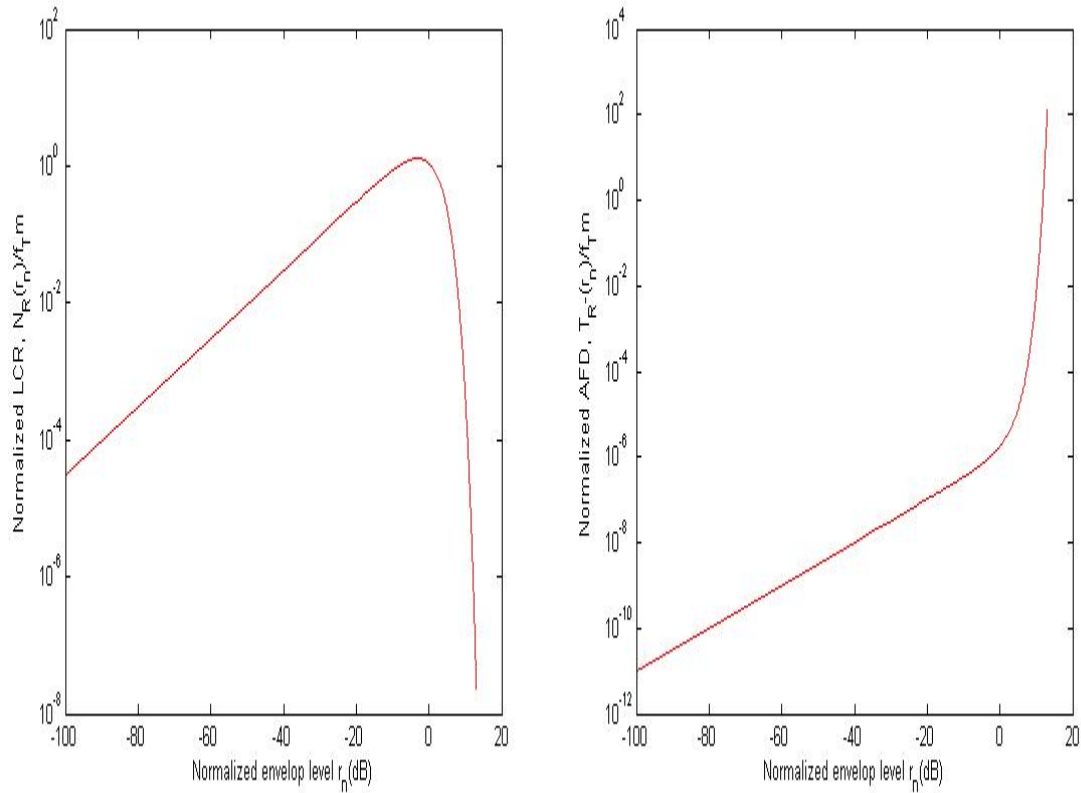


Figure 4.2.2 LCR and AFD $k_T = k_R = 3, \mu_T = 0, \mu_R = \pi$ non isotropic scattering environment.

If the signal is on average much stronger than the threshold, the number of threshold crossings (i.e., deep fades) is relatively small. Also if the signal is much weaker than the threshold, the number of crossings is small because signal "up-fades" are unlikely.

4.2.3 LCR and AFD $k_T = k_R = 3, \mu_T = \mu_R = \pi/2$ non isotropic environment

The parameters used for this numerical analysis:

$$f_c = 5.9\text{GHz}, f_{T_{\max}} = f_{R_{\max}} = 570\text{Hz}, \beta_T = \pi/3, \beta_R = \pi/4, a = 400\text{m}, D = 600\text{m}$$

$$\gamma_T = 0, \gamma_R = \pi, \mu_T = \mu_R = \pi/2, K_{pq} = 5$$

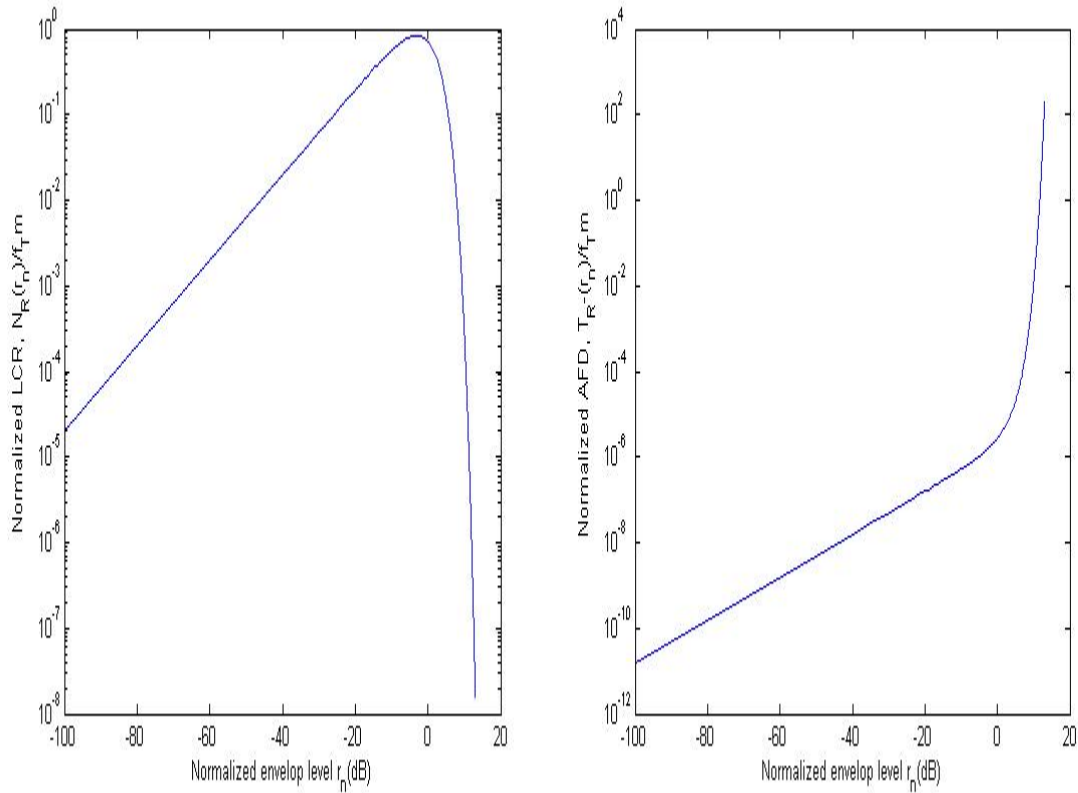


Figure 4.2.3 LCR and AFD $k_T = k_R = 3, \mu_T = \mu_R = \pi/2$ non isotropic scattering environment.

In this figure the angle spreads (related to the values of k_T and k_R), mean angled (related to the values of μ_T and μ_R), are the same $k_T = k_R = 3, \mu_T = \mu_R = \pi/2$. The result is a slight attenuation in the Level Crossing Rate if compared with the figure 4.2.2, where the parameters for the mean value are $\mu_T = 0, \mu_R = \pi$.

4.3 LCR and AFD of the MIMO M2M model for different Ricean factors

Normalized LCR and AFD of the MIMO M2M model for different Ricean factors

$$k_{pq} = 0, k_{pq} = 1, k_{pq} = 5 \text{ and } (k_T = k_R = 1, \gamma_T = 0, \gamma_R = \pi).$$

The influence of the Ricean factor k_{pq} and ratio factor s (s is the ratio of the maximum Doppler frequency $f_{R\max}$ and $f_{T\max}$, $s = f_{R\max} / f_{T\max}$) for a non-isotropic M2M channel on the LCR and AFD. The fades are shallower when k_{pq} is larger or s is smaller. Furthermore, the AFD tends to be larger when k_{pq} is larger or s is smaller.

4.3.1 LCR and AFD $k_{pq} = 0$ non isotropic environment

The parameters used for this numerical analysis:

$$f_c = 5.9\text{GHz}, f_{T\max} = f_{R\max} = 570\text{Hz}, \beta_T = \pi / 3, \beta_R = \pi / 4, a = 400\text{m}, D = 600\text{m}$$

$$\gamma_T = 0, \gamma_R = \pi, \mu_T = 0, \mu_R = \pi, k_T = k_R = 1,$$

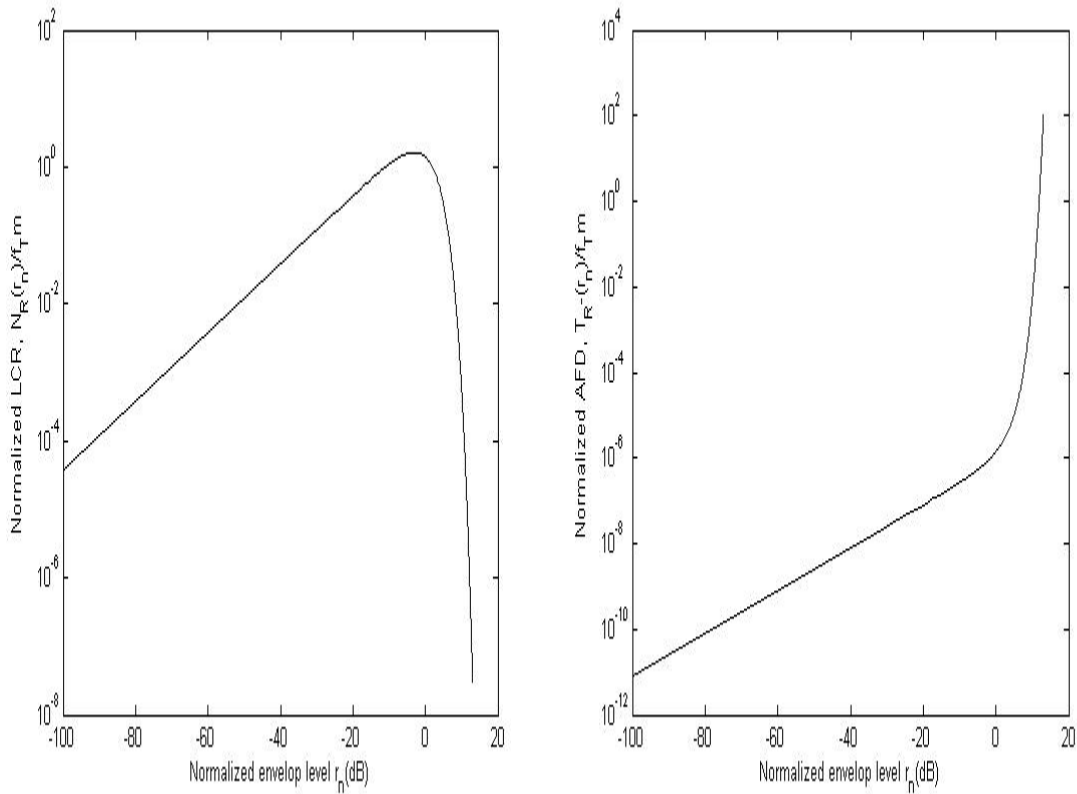


Figure 4.3.1 LCR and AFD $k_{pq} = 0$ and $(k_T = k_R = 1, \gamma_T = 0, \gamma_R = \pi)$ non isotropic scattering environment.

4.3.2 LCR and AFD $k_{pq} = 1$ non isotropic environment

The parameters used for this numerical analysis:

$$f_c = 5.9\text{GHz}, f_{T_{\max}} = f_{R_{\max}} = 570\text{Hz}, \beta_T = \pi / 3, \beta_R = \pi / 4, a = 400\text{m}, D = 600\text{m}$$

$$\gamma_T = 0, \gamma_R = \pi, \mu_T = 0, \mu_R = \pi, k_T = k_R = 1,$$

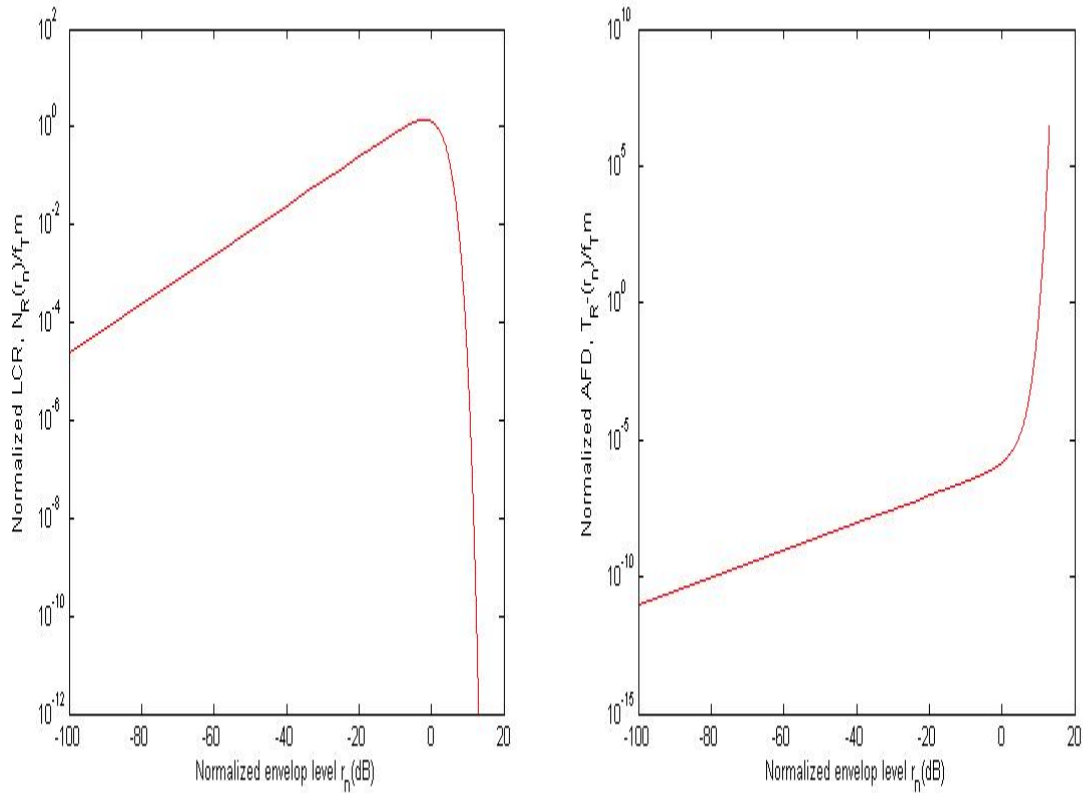


Figure 4.3.2 LCR and AFD $k_{pq} = 1$ and $(k_T = k_R = 1, \gamma_T = 0, \gamma_R = \pi)$ non isotropic scattering environment.

In this figure the Ricean factor k_{pq} is equal to one, comparing to the plot in figure 4.3.1 where the k_{pq} is zero, it is possible to observe that the AFD is slightly larger.

4.3.3 LCR and AFD $k_{pq} = 5$ non isotropic environment

The parameters used for this numerical analysis:

$$f_c = 5.9\text{GHz}, f_{T_{\max}} = f_{R_{\max}} = 570\text{Hz}, \beta_T = \pi / 3, \beta_R = \pi / 4, a = 400\text{m}, D = 600\text{m}$$

$$\gamma_T = 0, \gamma_R = \pi, \mu_T = 0, \mu_R = \pi, k_T = k_R = 1,$$

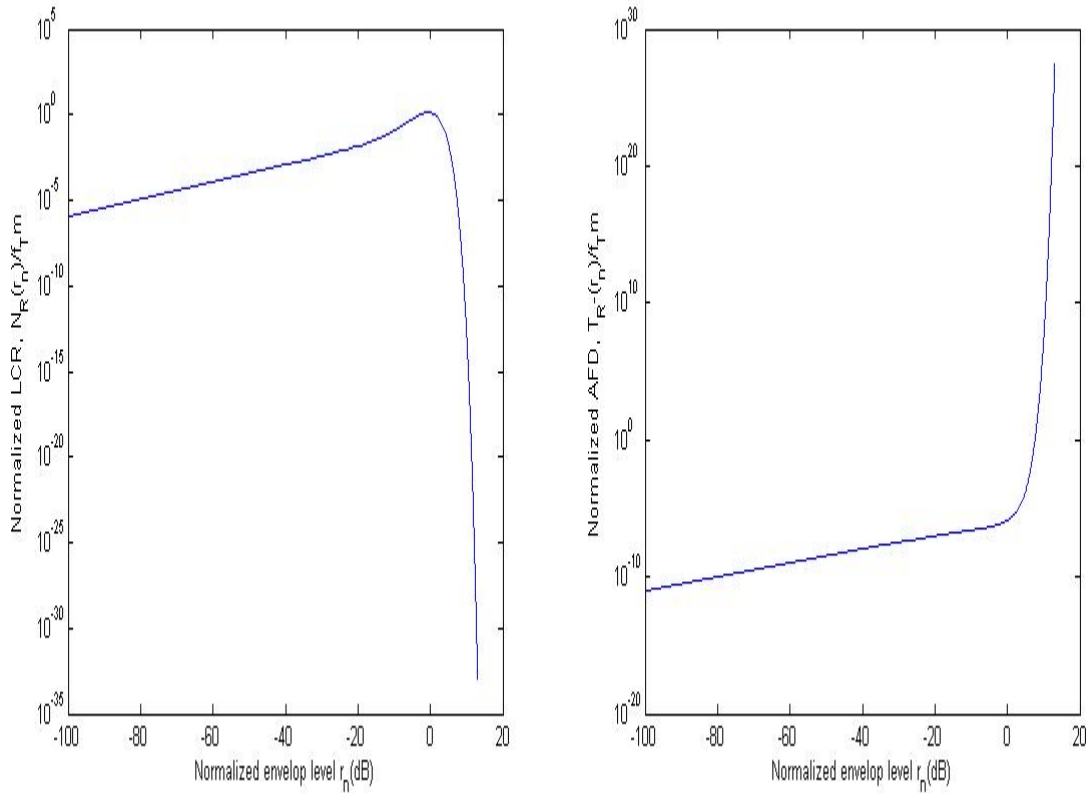


Figure 4.3.3 LCR and AFD $k_{pq} = 5$ and $(k_T = k_R = 1, \gamma_T = 0, \gamma_R = \pi)$ non isotropic scattering environment.

In this figure the k_{pq} is bigger and as consequence the fades are shallower, this effect can be observed if we compare to the figures where the k_{pq} is minor. In the AFD plot, the plot tends to be larger when k_{pq} is larger.

5 Conclusion and future work

5.1 Conclusion

In this study, the influence of the different physical parameters that determine a Multiple Input Multiple Output (MIMO) Mobile to Mobile (M2M) Elliptical ring channel were mathematically modeled and analyzed.

In this study, in order to test and analyze the Statistical properties of the mathematical model, a **GUI - Simulation Environment** was developed for the MIMO M2M Elliptical ring model.

The ST CF and the corresponding SD PSD for 2D non isotropic scattering environments are derived. Based on the obtained Doppler PSD for the elliptical ring model with single bounced rays and observations in [11], can be conclude that no matter what the propagation environment is, for M2M channels in non isotropic scattering environments, the single bounced rays will cause a Doppler PSD similar to the U shape.

The second order statistics of the non-isotropic MIMO M2M Ricean fading channel are considered and the analytical expressions for the LCR and AFD have been derived. Based on the derived LCR and AFD some important parameters were investigated in more detail.

The numerical simulations have revealed that the LCR and AFD are very sensitive to the angle spreads (K_T^{SB}, K_R^{SB}) , mean values (μ_T^{SB}, μ_R^{SB}) of the AoA ϕ_R^{SB} and AoD ϕ_T^{SB} , and directions of motion $(\gamma_T$ and $\gamma_R)$ in non-isotropic scattering environments.

5.2 Future work

These obtained interesting observations and analysis can be considered as useful guidance for further proposing more realistic MIMO M2M channel models.

The extension of the study for the MIMO M2M into wideband channel modelling.

References

- [1] A. S. Akki and F. Haber, "A statistical model for mobile-to-mobile land communication channel," *IEEE Trans. Veh. Technol.*, vol. VT-35, no. 1, pp. 2–7, Feb. 1986.
- [2] A. S. Akki, "Statistical properties of mobile-to-mobile land communication channels," *IEEE Trans. Veh. Technol.*, vol. 43, no. 4, pp. 826–831, Nov. 1994.
- [3] Gordon L. Stüber, "Principles of Mobile Communication", 2nd edition, Kluwer Academic Publishers, Boston, 2001. Chapter 2: Propagation modelling
- [4] C. S. Patel, G. L. Stüber, and T. G. Pratt, "Simulation of Rayleigh faded mobile-to-mobile communication channels," *IEEE Trans. Commun.*, vol.53, no. 11, pp. 1876-1884, Nov. 2005.
- [5] G. Acosta, K. Tokuda, and M. A. Ingram, "Measured joint Dopplerdelay power profiles for vehicle-to-vehicle communications at 2.4 GHz," in *Proc. IEEE Global Telecommun. Conf.*, vol. 6, Dallas, TX, Nov. 2004, pp. 3813–3817.
- [6] G. Acosta and M.A. Ingram, "Six Time- and Frequency-Selective Empirical Channel Models for Vehicular Wireless LANs," 1st IEEE International Symposium on Wireless Vehicular Communications, Sept 30 - Oct 1, 2007.
- [7] P. Almers, and E. Bonek, etc., "Survey of Channel and Radio Propagation Models for Wireless MIMO Systems," *EURASIP Journal on Wireless Communications and Networking*, vol. 2007, pp. 1–19, 2007.
- [8] Cheng-Xiang Wang, Xuemin Hong, Hanguang Wu, and Wen Xu, "Spatial temporal correlation properties of the 3GPP spatial channel model and the Kronecker MIMO channel model", *EURASIP Journal on Wireless Communications and Networking, Special Issue on Space-Time Channel Modelling for Wireless Communications*, vol. 2007, Article ID 39871, 9 pages, 2007. doi:10.1155/2007/39871.
- [9] K. . Ebruke, "A study on geometrially-based stochastic MIMO channel models," Master thesis, 2007.
- [10] X. Cheng, C.-X. Wang, and D. I. Laurenson, "Space-time-frequency characterization of non-isotropic MIMO mobile-to-mobile multicarrier Ricean fading channels," *IEEE IWCMC'08*, Chania Crete Island, Greece, submitted for publication.
- [11] X. Cheng, C.-X. Wang, and D. I. Laurenson, "A generic geometrical-based

- MIMO mobile-to-mobile channel model,” *IEEE IWCMC'08*, Chania Crete Island, Greece, submitted for publication.
- [12] A. G. Zajic and G. L. Stuber, “Space-Time Correlated MIMO Mobile-To-Mobile Channels,” in *Proc. of IEEE PIMRC2006*, Helsinki, Finland, Sep. 2006, pp.1-5.
- [13] A. G. Zajic and G. L. Stuber, “Three-Dimensional Modelling, Simulation and Capacity Analysis of Space-Time Correlated Mobile-to-Mobile Channels,” *IEEE Trans. Veh. Technol.*, to be published.
- [14] A. Paier, J. Karedal, N. Czink, H. Hofstetter, C. Dumard, T. Zemen, F. Tufvesson, C. F. Mecklenbräuker, and A. F. Molisch, “First results from car-to-car and car-to-infrastructure radio channel measurements at 5.2 GHz,” in *COST2100*, Duisburg, Germany, September 10-12, 2007, pp. 1 – 13.
- [15] Wikipedia MIMO in wireless communications, <http://en.wikipedia.org/wiki/MIMO>
- [16] A. Constantinides, and A. Shacham, “MIMO Wireless Systems”, May 14 2004, <http://www.columbia.edu/~acc40/MIMO.pdf>.
- [17] Matthias Pätzold and Bjørn Olav Hogstad, “A Wideband MIMO Channel Model Derived From the Geometric Elliptical Scattering Model,” *Proc. 3rd International Symposium on Wireless Communication System, ISWCS'06*, Valencia, Spain, Sept. 2006, pp. 138–143.
- [18] C. Oestges, B. Clerckx, D. Vanhoenacker-Janvier and A. J. Paulraj, “Impact of Fading Correlations on MIMO Communication Systems in Geometry-based statistical Channel Models”, *IEEE Transactions on Wireless Communications*, Vol 4, Issue 3, May 2005, pp. 1112 – 1120.
- [19] G. J. Byers and F. Takawira, “The influence of spatial and temporal correlation on the capacity of MIMO channels,” in *Wireless Communications and Networking 2003, WCNC 2003*, Mar. 2003, pp. 359–364.
- [20] J. Wallace and M. Jensen, “Statistical Characteristics of Measured MIMO Wireless Channel Data and Comparison to Conventional Models,” in *Proc. IEEE Vehicular Technology Conference, VTC 2001 Fall*, vol. 2, Sidney, Australia, Oct. 2001, pp. 1078–1082.
- [21] ———, “Modelling the Indoor MIMO Wireless Channel,” *IEEE Trans. on Antennas and Propagation*, vol. 50, no. 5, pp. 591–599, May 2002.
- [22] C.-N. Chuah, J. Kahn, and D. Tse, “Capacity of Multi-Antenna Array Systems in Indoor Wireless Environment,” in *Proc. IEEE Global Telecommunications Conf.*,

vol. 4, Sidney, Australia, 1998, pp. 1894–1899.

- [23] D. Chizhik, F. Rashid-Farrokhi, J. Ling, and A. Lozano, "Effect of Antenna Separation on the Capacity of BLAST in Correlated Channels," *IEEE Comm. Letters*, vol. 4, no. 11, pp. 337–339, Nov. 2000.
- [24] Rad, H.S., and Gazor, S., "A 3D correlation model for MIMO non-isotropic scattering with arbitrary antenna arrays", *Wireless Communications and Networking Conference, 2005 IEEE*, Vol.2, Iss., 13-17 March 2005 Pages: 938-943 Vol. 2
- [25] A. Alcocer-Ochoa, V.Y. Kontorovitch, and R. Parra-Michel, "Wideband MIMO Channel Model Based on Geometrical Approximations", *1st International Conference on Electrical and Electronics Engineering*, 24 -27 June 2004, pp. 29 -34
- [26] A. Constantinides, and A. Shacham, "MIMO Wireless Systems", May 14 2004, <http://www.columbia.edu/~acc40/MIMO.pdf>.

Appendices

Portable Document Format (PDF) version and
Matlab codes and figures

<http://www.amcomputersystems.com/vibot/vibots/mateos/index.html>